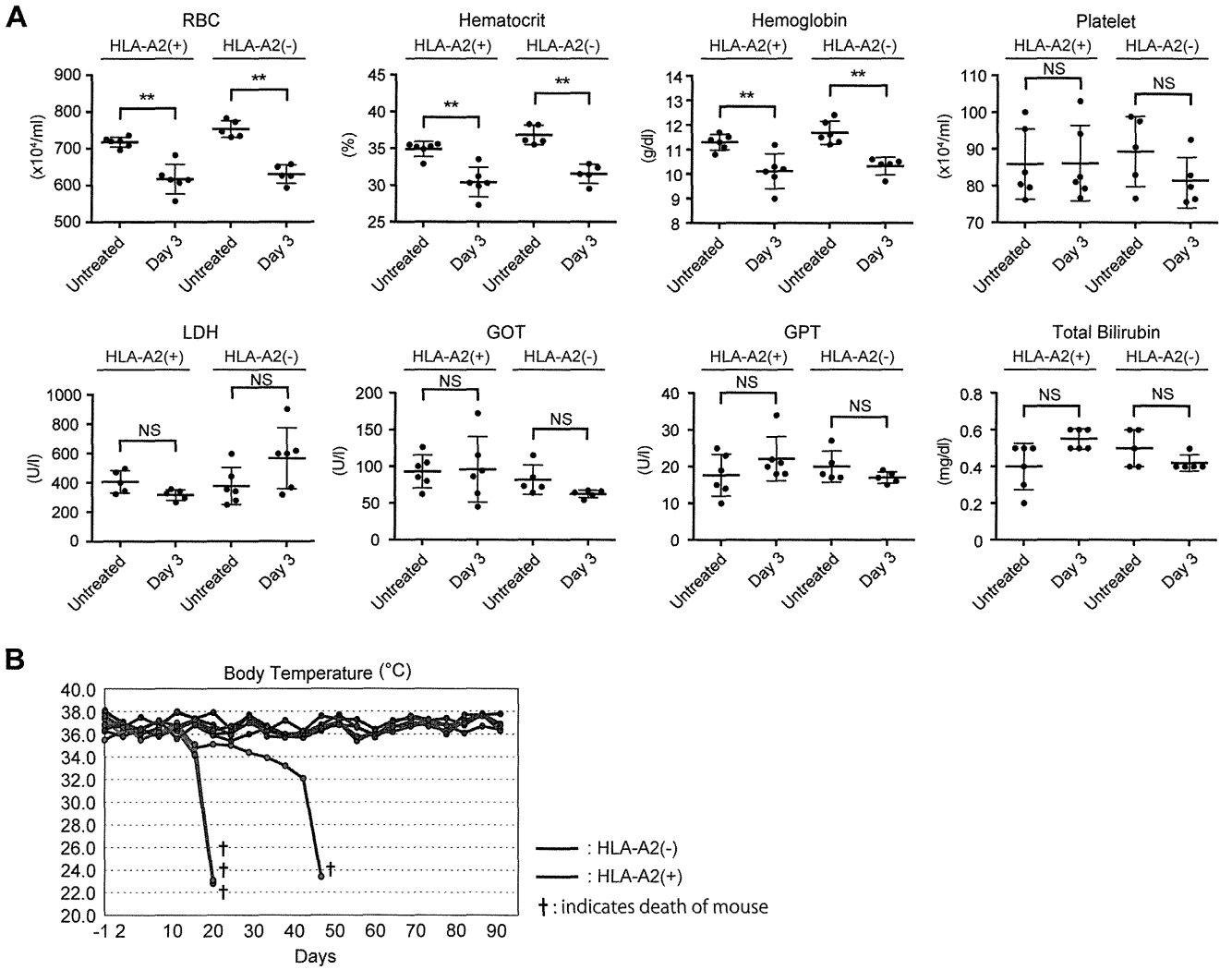

Supplementary Figure E3. Results of hematologic and biomarker studies of GVHD-model mice before and after kASHmAb treatment. (A) Blood was sampled from the retroorbital venous plexus and examined on days -1 (just before PBMC transplantation) and 3 (just before kASHmAb injection). We determined complete blood counts (CBC; hematocrit with red blood cell, hemoglobin, and platelet concentrations), serum total bilirubin concentration, LDH, GOT, and GPT activities in 5 HLA-A2(-) PBMC-transplanted mice and 6 HLA-A2(+) PBMC-transplanted mice. All mice were 7-8 weeks old. Paired t-test, $*P<0.05$; $**P<0.01$; NS: not significant. (B) Body temperature of GVHD-model mice before and after kASHmAb treatment [Red line; HLA-A2(-) PBMC-transplanted mice = GVHD(+), Blue line; HLA-A2(+) PBMC-transplanted mice = GVHD(-)]. Body temperature was determined twice weekly between 1500h and 1900h at room temperature 22°C and ambient humidity 55%. Percentage change from initial weight is shown. HLA = human leukocyte antigen; RBC = red blood cells; LDH = lactate dehydrogenase; GOT = glutamic oxaloacetic transaminase; GPT = glutamic pyruvic transaminase; GVHD = graft-versus-host disease; PBMC = peripheral blood mononuclear cell.

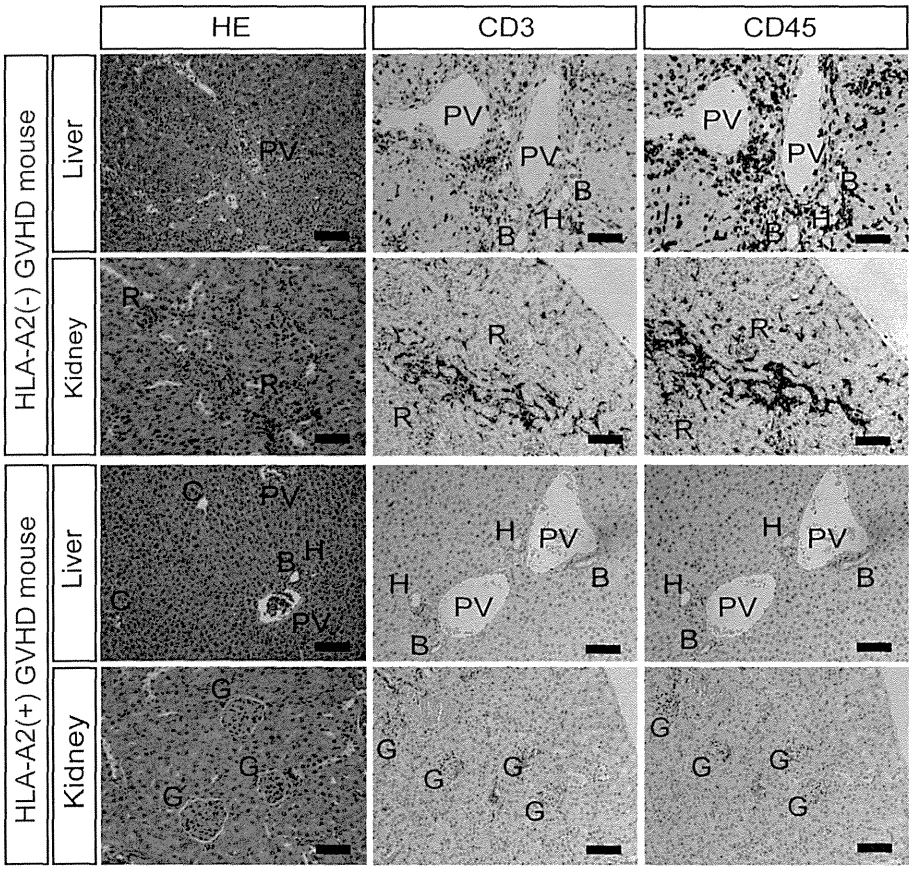

Supplementary Figure E4. Tissues from GVHD-model mice immunostained for human antigens (kidney and liver). Three weeks after transplantation, liver and kidneys were obtained from NOD/Shi-scid/IL-2Rγnull mice intravenously transplanted with human PBMCs [HLA-A2(-) or HLA-A2(+)]. Sections of routinely processed formalin-fixed, paraffin-embedded material were stained with anti-human CD3 and CD45 antibodies with 3,3'-diamino-benzidine (DAB) substrate as chromogen and hematoxylin as nuclear counterstain. While HLA-A2(+) GVHD mouse shows no human derived-cells, HLA-A2(-) GVHD mouse organs show human CD3 or CD45 cells; magnification, original image, x200, liver; x400, kidney). Scale bar 400 μm (kidney: 200 μm). B = Bile duct; C = Central vein; G = Glomerulus; GVHD = graft-versus-host disease; H = Hepatic artery; HE = hematoxylin and eosin; HLA = human leukocyte antigen; PBMC = peripheral blood mononuclear cell ; PV = Portal vein; R = Renal corpuscle.

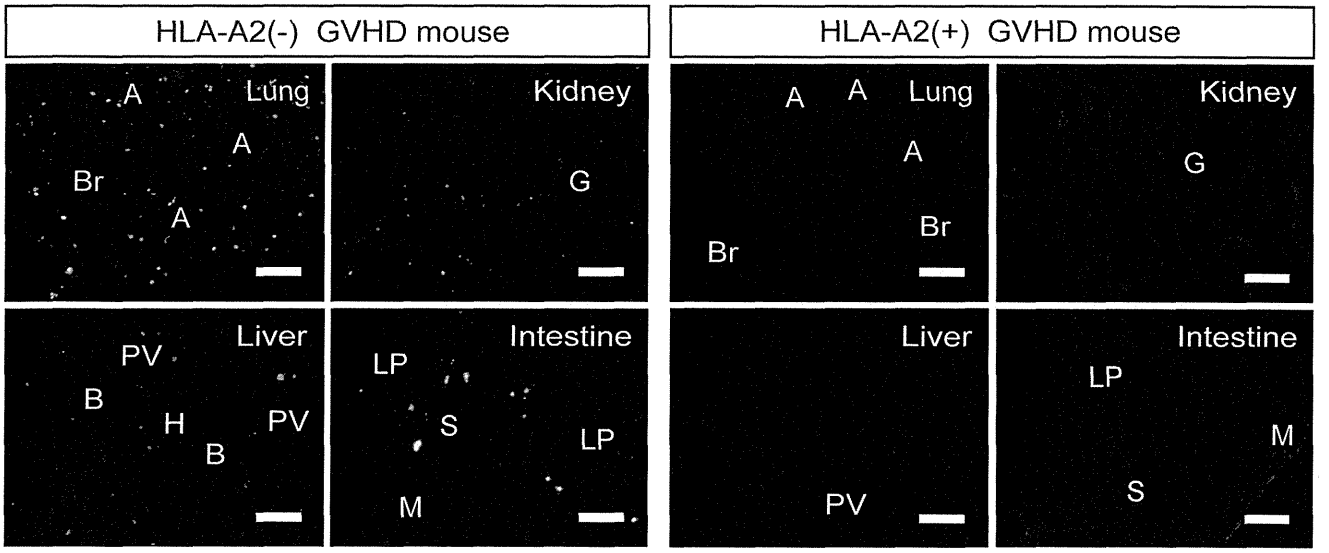

Supplementary Figure E5. Apoptosis in sections of organs of HLA-A2(-) and HLA-A2(+) GVHD-model mice after TdT-mediated dUTP nick end-labeling (TUNEL). Using routinely processed formalin-fixed, paraffin-embedded material, we evaluated apoptosis in sections of liver, lungs, intestine, and kidneys of HLA-A2(-) and HLA-A2(+) GVHD-model mice, obtained 3 weeks after transplantation, by light microscopy after TdT-mediated dUTP nick end-labeling. Green dots indicate apoptotic cells. Magnification, original images, x200. Scale bars 400 μm. A = Alveoli; B = Bile duct; Br = Bronchiole; G = Glomerulus; GVHD = graft-versus-host disease; H = Hepatic artery; HLA = human leukocyte antigen; LP = Lamina propria; M = Muscularis; PV = Portal vein; S = submucosa.

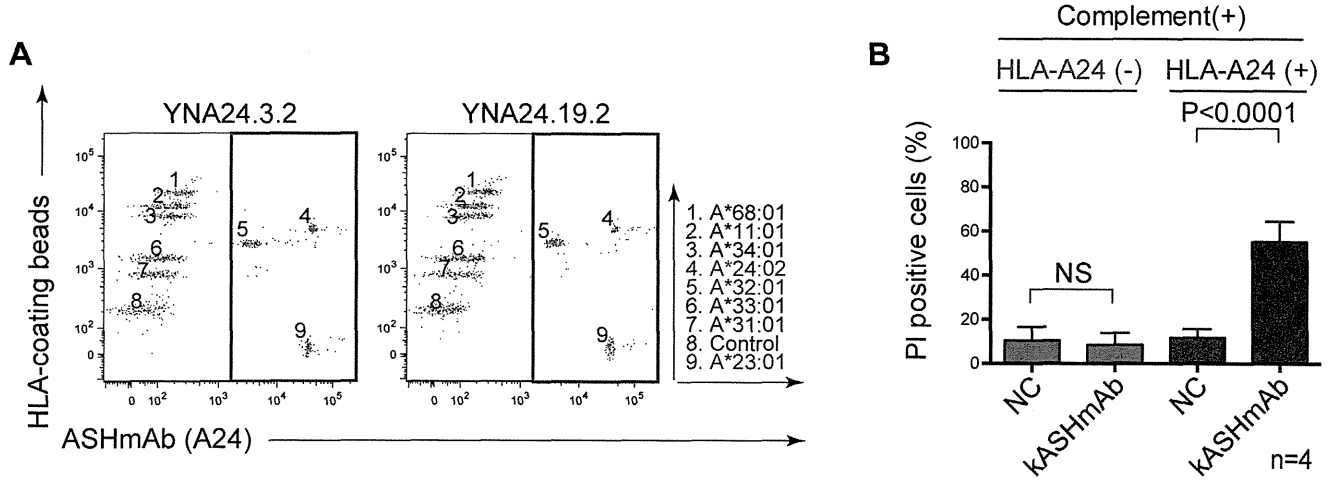

Supplementary Figure E6. Allele-specific cytotoxicity of HLA-A24-killing ASHmAb (in vitro). (A) To establish ASHmAb-producing clones, on day 28 hybridomas (Supplementary Fig. 1) selected as producing anti-HLA antibody at initial screening were secondarily screened with FlowPRA, using flow cytometry (YNA24.3.2 and YNA24.19.2). Hybridoma-culture supernatants were incubated with HLA-coated beads. After incubation, the beads were washed and stained with secondary antibodies. Bead fluorescence intensities were measured using a flow cytometer and specificities of anti-HLA monoclonal antibodies were determined. Representative flow cytometry data are shown for a combination of FlowPRA beads coated with HLA-A*68:01, A*11:01, A*34:01, A*24:02, A*32:01, A*33:01, A*31:01, and control antigen or A*23:01. (B) Statistical analysis of in vitro killing assay using A24 ASHmAb with baby-rabbit complement. HLA-A24(-) cells (red bar) and HLA-A2(+) cells (blue bar) from healthy donors were each cultured with isotype control or A24 ASHmAb hybridoma supernatant. Percentages of dead cells were determined by propidium iodide staining and flow cytometry. Doublets and dead cells were excluded from flow-cytometry data. NC; Negative control. NS; Not significant. Data shown as mean ± s.d (n=4, $p < 0.05$ by Student's t-test). ASHmAb = allele-specific anti-HLA monoclonal antibody; HLA = human leukocyte antigen; kASHmAb = killing ASHmAb; NC = negative control; NS = nonsignificant; PI = propidium iodide.

Leukemia & Lymphoma, 2014; Early Online: 1–3

ISSN: 1042-8194 print / 1029-2403 online
DOI: 10.3109/10428194.2014.949261

informa
healthcare

LETTER TO THE EDITOR

Single-unit cord blood transplant for acute lymphoblastic leukemia and lymphoma using an intensified conditioning regimen of total body irradiation, high-dose cytarabine and cyclophosphamide

Takaaki Konuma, Seiko Kato, Maki Oiwa-Monna, Arinobu Tojo & Satoshi Takahashi

Department of Hematology/Oncology, The Institute of Medical Science, The University of Tokyo, Tokyo, Japan

Cord blood transplant (CBT) from an unrelated donor has recently been utilized as an alternative transplant method for patients with lymphoid neoplasms when patients are without related and unrelated adult donors [1–6]. However, a high incidence of graft failure remains one of the major disadvantages in CBT for adult patients. The purpose of a conditioning regimen prior to allogeneic hematopoietic stem cell transplant (allo-HSCT) for malignant disease is disease eradication and immunosuppression to achieve graft engraftment. With regard to stable engraftment, an optimal conditioning regimen prior to CBT for adult patients with lymphoid neoplasms is yet to be determined. In the present study, we analyzed the results of CBT after an intensified conditioning regimen of total body irradiation (TBI), high-dose cytarabine (Ara-C) and cyclophosphamide (CY) in 32 adult patients with acute lymphoblastic leukemia (ALL) and non-Hodgkin lymphoma (NHL) with long-term follow-up.

This retrospective study included 32 consecutive adult patients who underwent unrelated allo-HSCT using single-unit cord blood (CB) for ALL or NHL at the Institute of Medical Science, The University of Tokyo between April 2004 and July 2013. Eleven patients had been included in our previous study [6], and extended the follow-up. The diagnosis of ALL and NHL was made according to the World Health Organization classification. CB units were obtained from the Japan Cord Blood Bank Network and selected as reported previously [7]. All patients received 12 Gy TBI in four divided fractions on days − 8 and − 7, Ara-C on days − 5 and − 4 (total dose 12 g/m^2, 3 g/m^2 every 12 h for 2 days) and CY (total dose 120 mg/kg) on days − 3 and − 2 as a conditioning regimen, and received cyclosporine A (3 mg/kg/day) with a short course of methotrexate (15 mg/m^2 on day + 1 and 10 mg/m^2 on days + 3 and + 6) as a graft-versus-host disease (GVHD) prophylaxis. Although 28 patients received one or more courses of prophylactic intrathecal chemotherapy before the conditioning regimen, no patients received it after CBT. The institutional review board of the Institute of Medical Science, The University of Tokyo approved this study, which was conducted in accordance with the Declaration of Helsinki.

The probability of overall survival (OS), which was defined as the time from the date of CBT to the date of death or last contact, was estimated according to the Kaplan–Meier method. The probabilities of relapse, which was defined by morphologic evidence of disease in peripheral blood, bone marrow or extramedullary sites, and transplant-related mortality (TRM), which was defined as death during remission, were estimated based on a cumulative incidence method to accommodate competing risks. Univariate analysis was performed with a Cox regression model for OS and the Fine and Gray regression model for relapse and TRM. The following variables were considered: patient age (<40 vs. ≥ 40 years), disease type (ALL vs. NHL), disease status at CBT (standard risk vs. high risk), cord blood nucleated cell count (<2.5 vs. $\geq 2.5 \times 10^7$/kg), cord blood CD34 + cell count ($<1 \times 10^5$/kg vs. $\geq 1 \times 10^5$/kg), human leukocyte antigen (HLA) disparities based on HLA-A and -B antigen level and HLA-DRB1 allele level (≤ 2 vs. ≥ 3), sex compatibility (female donor to male recipient vs. other) and ABO compatibility (match vs. mismatch). Since the number of patients was small, we were unable to perform multivariate analysis to identify variables influencing outcomes. All statistical analyses were performed with EZR (Saitama Medical Center, Jichi Medical University, Saitama, Japan), a graphical user interface for R 3.0.2 (R Foundation for Statistical Computing, Vienna, Austria) [8]. Analysis of data was performed in April 2014.

The characteristics of patients, CB units and transplant procedures are shown in Table I. The median age was 39 years (range, 18–49 years), the median number of nucleated cells was 2.60×10^7/kg (range, 1.65–5.69 $\times 10^7$/kg) and the median number of CD34 + cells was 0.94×10^5/kg (range, 0.41–2.81 $\times 10^5$/kg). Disease types were ALL in 27 patients, and NHL in five. Among patients with ALL, 11 patients had the Philadelphia chromosome abnormality. All patients achieved neutrophil and platelet recovery after CBT. The median time to more than 0.5×10^9/L absolute neutrophil

Correspondence: Takaaki Konuma, Department of Hematology/Oncology, The Institute of Medical Science, The University of Tokyo, 4-6-1, Shirokanedai, Minato-ku, Tokyo 108-8639, Japan. Tel: + 81-3-3443-8111. Fax: + 81-3-5449-5429. E-mail: tkonuma@ims.u-tokyo.ac.jp

Received 3 July 2014; revised 18 July 2014; accepted 22 July 2014

Table I. Characteristics of patients, cord blood units and transplants.

Characteristic	Value
Number of patients	32
Sex, number (%)	
Male	18 (56)
Female	14 (43)
Age, years, median (range)	39 (18–49)
CMV serostatus, number (%)	
Positive	27 (84)
Negative	5 (15)
Disease type/disease status at CBT, number (%)	
ALL*	27 (84)
CR1	19
CR2	4
CR3	2
CR4	1
Refractory relapse	1
NHL†	5 (15)
CR1	2
CR3	1
Refractory relapse	2
Number of nucleated cells, $\times 10^7$/kg, median (range)	2.60 (1.65–5.69)
Number of CD34 + cells, $\times 10^5$/kg, median (range)	0.94 (0.41–2.81)
HLA disparities‡, number (%)	
1	4 (12)
2	18 (56)
3	10 (31)
ABO incompatibility, number (%)	
Match	9 (28)
Major mismatch	12 (37)
Minor mismatch	9 (28)
Bidirectional mismatch	2 (6)
Sex incompatibility, number (%)	
Female donor to male recipient	9 (28)
Other	23 (71)

CMV, cytomegalovirus; CBT, cord blood transplant; ALL, acute lymphoblastic leukemia; CR; complete remission; NHL, non-Hodgkin lymphoma; HLA, human leukocyte antigen.
*Eleven patients had Philadelphia chromosome abnormality.
†Five patients with NHL included diffuse large B-cell lymphoma ($n = 2$), B-cell lymphoma, unclassifiable ($n = 1$), adult T-cell leukemia/lymphoma ($n = 1$) and peripheral T-cell lymphoma ($n = 1$).
‡Number of HLA disparities, defined as low resolution for HLA-A and -B and high resolution for HLA-DRB1.

count was 21 days (range, 17–46 days). The median time to untransfused platelet count greater than 50×10^9/L was 41 days (range, 32–204 days). All patients showed durable complete donor chimerism after CBT. The cumulative incidence of grade III–IV acute GVHD and extensive chronic GVHD was 6.2% (95% confidence interval [CI], 1.1–18.4%) at 100 days and 23.4% (95% CI, 10.0–40.0%) at 3 years after CBT, respectively. At a median follow-up of survivors of 46.5 months (range, 3–118 months), the probability of OS at 5 years was 71.6% (95% CI, 47.9–85.9%) [Figure 1(A)]. The cumulative incidence of relapse at 5 years was 19.4% (95% CI, 7.7–35.0%) [Figure 1(B)]. No TRM was observed during the first 100 days. The cumulative incidences of TRM at 1 year and 3 years were 3.2% (95% CI, 0.2–14.4%) and 6.6% (95% CI, 1.1–19.3%), respectively [Figure 1(C)]. In univariate analysis, no factors were associated with overall mortality and relapse incidence. The causes of death were relapse in four patients, chronic GVHD in two patients, post-transplant lymphoproliferative disease in one patient and donor-derived myelodysplastic syndrome in one patient.

We evaluated the effect of the addition of Ara-C to TBI/CY prior to CBT for patients with lymphoid neoplasms. Durable engraftment and complete donor chimerism were achieved in all patients, although one of the major disadavantages in CBT is a high incidence of graft failure. Furthermore, no patients developed early TRM after CBT, although regimen-related toxicities could not be evaluated. These data suggested that the addition of Ara-C to TBI/CY could provide durable engraftment of single-unit CB without increased toxicities in our cohort.

The prognosis of adult patients with lymphoid neoplasms has been less favorable because of high rates of relapse even after allo-HSCT from related and unrelated adult donors conditioned with TBI/CY, which is the most useful myeloablative conditioning regimen for patients with lymphoid neoplasms. In order to decrease relapse, the effect of intensified conditioning regimens has been analyzed in several studies [9–13]. Although the addition of etoposide (VP-16) or Ara-C to a TBI/CY conditioning regimen has been reported to be safely and effectively used for patients with ALL [9,10], most of the studies did not show any advantage of intensified conditioning regimens to improve outcome [11–13]. However, the majority of these studies did not analyze patients receiving CBT. In our study, although the disease status in 29 of 32 patients (90.6%) was complete remission at the time of CBT, the cumulative incidence of relapse at 5 years was 19.4% after CBT. Since relapse might depend on disease type or status at the time of allo-HSCT, whether the addition of Ara-C to the TBI/CY conditioning regimen reduces post-transplant relapse after CBT should be confirmed in prospective studies.

In conclusion, although this study was a retrospective single-institution analysis in Japan and the number of patients was small, an intensified conditioning regimen of TBI, Ara-C

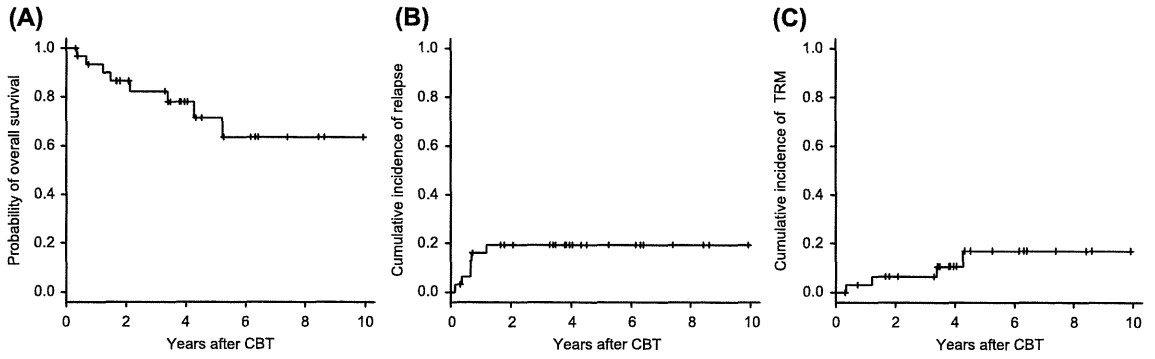

Figure 1. Probability of overall survival and cumulative incidences of relapse and transplant-related mortality (TRM) after CBT following TBI/Ara-C/CY. Overall survival (A), relapse (B) and TRM (C) in 32 patients with ALL or NHL after CBT following TBI/Ara-C/CY.

and CY prior to CBT might be safe and effective in adult patients with ALL and NHL.

Potential conflict of interest: Disclosure forms provided by the authors are available with the full text of this article at www.informahealthcare.com/lal.

References

[1] Kumar P, Defor TE, Brunstein C, et al. Allogeneic hematopoietic stem cell transplantation in adult acute lymphocytic leukemia: impact of donor source on survival. Biol Blood Marrow Transplant 2008;14:1394–1400.
[2] Tomblyn MB, Arora M, Baker KS, et al. Myeloablative hematopoietic cell transplantation for acute lymphoblastic leukemia: analysis of graft sources and long-term outcome. J Clin Oncol 2009;27:3634–3641.
[3] Atsuta Y, Suzuki R, Nagamura-Inoue T, et al. Disease-specific analyses of unrelated cord blood transplantation compared with unrelated bone marrow transplantation in adult patients with acute leukemia. Blood 2009;113:1631–1638.
[4] Marks DI, Woo KA, Zhong X, et al. Unrelated umbilical cord blood transplant for adult acute lymphoblastic leukemia in first and second complete remission: a comparison with allografts from adult unrelated donors. Haematologica 2014;99:322–328.
[5] Rodrigues CA, Rocha V, Dreger P, et al. Alternative donor hematopoietic stem cell transplantation for mature lymphoid malignancies after reduced-intensity conditioning regimen: similar outcomes with umbilical cord blood and unrelated donor peripheral blood. Haematologica 2014;99:370–377.
[6] Ooi J, Takahashi S, Tomonari A, et al. Unrelated cord blood transplantation after myeloablative conditioning in adults with ALL. Bone Marrow Transplant 2009;43:455–459.
[7] Takahashi S, Ooi J, Tomonari A, et al. Comparative single-institute analysis of cord blood transplantation from unrelated donors with bone marrow or peripheral blood stem-cell transplants from related donors in adult patients with hematologic malignancies after myeloablative conditioning regimen. Blood 2007;109:1322–1330.
[8] Kanda Y. Investigation of the freely available easy-to-use software "EZR" for medical statistics. Bone Marrow Transplant 2013;48:452–458.
[9] Shigematsu A, Kondo T, Yamamoto S, et al. Excellent outcome of allogeneic hematopoietic stem cell transplantation using a conditioning regimen with medium-dose VP-16, cyclophosphamide and total-body irradiation for adult patients with acute lymphoblastic leukemia. Biol Blood Marrow Transplant 2008;14:568–575.
[10] Mori T, Aisa Y, Kato J, et al. Safety and efficacy of total body irradiation, cyclophosphamide, and cytarabine as a conditioning regimen for allogeneic hematopoietic stem cell transplantation in patients with acute lymphoblastic leukemia. Am J Hematol 2012;87:349–353.
[11] Mengarelli A, Iori A, Guglielmi C, et al. Standard versus alternative myeloablative conditioning regimens in allogeneic hematopoietic stem cell transplantation for high-risk acute leukemia. Haematologica 2002;87:52–58.
[12] Kanda Y, Sakamaki H, Sao H, et al. Effect of conditioning regimen on the outcome of bone marrow transplantation from an unrelated donor. Biol Blood Marrow Transplant 2005;11:881–889.
[13] Inamoto Y, Nishida T, Suzuki R, et al. Significance of additional high-dose cytarabine in combination with cyclophosphamide plus total body irradiation regimen for allogeneic stem cell transplantation. Bone Marrow Transplant 2007;39:25–30.

BLOOD RESEARCH
Volume 49 · Number 4 · December 2014
http://dx.doi.org/10.5045/br.2014.49.4.209

Editorial

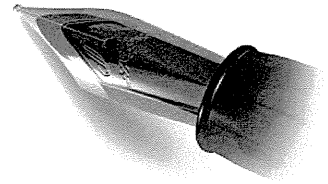

Here comes the cord

Satoshi Takahashi, M.D., Ph.D.

Adult Hematopoietic Stem Cell Transplant Program, Division of Molecular Therapy, Advanced Clinical Research Center, Institute of Medical Science, University of Tokyo, Tokyo, Japan

Hematopoietic stem cell transplantation has been established as a lifesaving therapy for leukemias or other hematopoietic malignancies since more than a half century ago [1]. Human leukocyte antigen (HLA)-matched sibling is the preferred donor for the better clinical outcomes, whiles, even patients without suitable family donor could also receive the benefits from unrelated donor registries or cord blood (CB) banks. International collaboration has also been well-improved in this field. Nowadays, almost all patients who need allogeneic transplantation are able to find adequate donors.

Advantages to use CB unit are the quick availability, lower risk of severe graft-versus-host disease (GVHD) even though HLA between recipients and CB grafts is mismatched in most cases, and no risk for CB donors medically and mentally. Since the first patient received the CB from his HLA-matched sister to treat Fanconi Anemia successfully in 1988 [2], many CB banks have been established and the numbers of transplants using unrelated CB units dramatically increased. There are approximately 621,000 CB units in the database of Bone Marrow Donors Worldwide (BMDW: http://www.bmdw.org/). Recently, more than 3,000 CB transplantation (CBT)s are carried out annually all over the world: one third in Europe, one third in North America and another one third in Asia (mostly in Japan). Pediatric patients were major users in early period, however, CBT are gradually adopted in adults in this decade. For example, we are performing more than 1,200 transplantations using single CB unit annually in Japan, and more than 80% are adult patients with hematology malignancies, and a half of the recipients are older than 50 years. The major reason of this increment in the world is the improved clinical outcomes. Recently, for example, Eapen and colleagues [3] compared results of 165 single CBT for adult patients, 888 peripheral blood stem cell transplant (PBSCT) patients, and 472 bone marrow transplant (BMT) patients. Transplant-related mortality was higher for the CBT patients, but chronic GVHD were lower. Leukemia-free survival was comparable among CBT, fully matched, and mismatched PBSCT/BMT patients [3]. These findings have contributed to increase the CBT activity among the international transplant societies and have gradually improved the reliability of this transplant strategy.

There is still limitation in CBT such as delayed engraftment and poor immune cell reconstitution [4]. The quality assurance of CB unit is also key issue for the reliability of CBT among the patients, their families, and transplant physicians. Cell dose is the most significant parameters for engraftment capacity of CB unit and also for survival results after CBT. Especially, CD34-positive cell number indicates the hematopoietic stem or progenitor cell function. However, the diversity of technical difference between CB banks has been evoked and it is necessary that we adjust that standard. Efforts are being intensified by the Foundation for the Accreditation of Cellular Therapy and the Joint Accreditation Committee - International Society for Cellular Therapy and European Group for Blood and Marrow Transplantation (FACT-JACIE), the American Association

of Blood Banks (AABB), and CB banks all over the world. Because the importance of cell dose is critical, researchers are focusing on CB expansion strategies and some of them are under laboratory and clinical assessment.

Under the situation described as above, CBT is definitely contributing to improving the life prognosis of patients with hematological malignancies. On the other hand, the utilized percentage of donated CB units all over the world is 6.3% reported by World Marrow Donor Association (WMDA), however it was reported as 1.2% in Korea. In this issue of **Blood Research**, Choi *et al.* [5] has analyzed the reasons by the questionnaire survey using "Audience Response System" for 67 board-certified transplant physicians at the annual meeting of the Korean Society of Blood and Marrow Transplantation. According to ordinary expectations, Korean physicians are now not positive for choose CB units as stem cell source for transplantation, because of the fears for poor clinical results and for unsatisfied quality of CB units from domestic CB banks. However, some Korean transplant specialists and CB bank persons have continued to proceed with great efforts for achieving the satisfied clinical outcomes with CBT and for obtaining good enough quality of CB units. They have already known the education is also important to improve the reliabilities for the strategy. Please just remember the time when you started BMT or PBSCT, or even transplant with haplo just a couple of years ago. Nothing gains without going forward. Here comes the time of CBT.

REFERENCES

1. Appelbaum FR. Hematopoietic-cell transplantation at 50. N Engl J Med 2007;357:1472-5.
2. Gluckman E, Broxmeyer HA, Auerbach AD, et al. Hematopoietic reconstitution in a patient with Fanconi's anemia by means of umbilical-cord blood from an HLA-identical sibling. N Engl J Med 1989;321:1174-8.
3. Eapen M, Rocha V, Sanz G, et al. Effect of graft source on unrelated donor haemopoietic stem-cell transplantation in adults with acute leukaemia: a retrospective analysis. Lancet Oncol 2010; 11:653-60.
4. Ballen KK, Gluckman E, Broxmeyer HE. Umbilical cord blood transplantation: the first 25 years and beyond. Blood 2013;122: 491-8.
5. Choi BS, Mun YC, Kim JY, Lee YH. Perceptions of cord blood transplantation among transplant physicians in Korea: a questionnaire survey. Blood Res 2014;49:228-33.

Leukemia Research Reports 3 (2014) 54–57

Contents lists available at ScienceDirect

Leukemia Research Reports

journal homepage: www.elsevier.com/locate/lrr

Case report

Identification of a novel *SEPT9-ABL1* fusion gene in a patient with T-cell prolymphocytic leukemia

Rikio Suzuki [a,e], Hiromochi Matsushita [b,c], Hidetsugu Kawai [a,c], Hideyuki Matsuzawa [c,d], Kosuke Tsuboi [a], Shigeki Watanabe [e], Hiroshi Kawada [a,c], Yoshiaki Ogawa [a], Kiyoshi Ando [a,c,*]

[a] Division of Hematology/Oncology, Department of Internal Medicine, Tokai University School of Medicine, Isehara, Kanagawa, Japan
[b] Department of Laboratory Medicine, Tokai University School of Medicine, Isehara, Kanagawa, Japan
[c] Research Center for Cancer Stem Cell, Tokai University School of Medicine, Isehara, Kanagawa, Japan
[d] Teaching and Research Support Center, Tokai University School of Medicine, Isehara, Kanagawa, Japan
[e] Division of Hematology, Ebina General Hospital, Ebina, Kanagawa, Japan

ARTICLE INFO

Article history:
Received 6 March 2014
Received in revised form
15 June 2014
Accepted 16 June 2014
Available online 28 June 2014

Keywords:
T-cell prolymphocytic leukemia
SEPT9-ABL1
Tyrosine kinase inhibitors

ABSTRACT

T-cell prolymphocytic leukemia (T-PLL), a rare type of peripheral T-cell leukemia, is characterized by marked splenomegaly with rapidly progressive lymphocytosis and a poor prognosis. Nine kinds of *ABL1* chimeric genes have been identified in various kinds of hematological malignancies, such as chronic myeloid leukemia and B- or T-lymphoblastic leukemia. However, there have been no reports describing T-PLL cases with *ABL1* rearrangements. We herein report a case of T-PLL with a novel *SEPT9-ABL1* fusion gene which induced strong resistance to tyrosine kinase inhibitors such as imatinib and dasatinib.

1. Introduction

T-cell prolymphocytic leukemia (T-PLL) is a rare type of peripheral T-cell leukemia with a naive T-cell phenotype [1]. The clinical features of T-PLL include marked hepatosplenomegaly and generalized lymphadenopathy with rapidly progressive lymphocytosis. The prognosis is generally poor due to resistance to chemotherapy, with a median survival ranging from 7.5 to 50 months [1–3]. Chromosomal abnormalities such as t(14;14)(q11;q32), inv(14)(q11;q32) and t(X;14)(q28;q11) have been identified in patients with T-PLL, which result in the rearrangement of the *TCL1* or *MTCP1* genes with the T-cell receptor loci, which were thought to contribute to the pathogenesis of T-PLL [3].

We herein report a case of T-PLL with a novel *ABL1* fusion gene which was fused to *SEPT9*, *SEPT9-ABL1*. The case exhibited strong resistance to the tyrosine kinase inhibitors (TKI) used against *BCR-ABL1*. This is the first report of T-PLL with an *ABL1* fusion gene, and additionally, only the second report of a hematological malignancy with an *ABL1* fusion gene that exhibited a poor response to TKI.

2. Case report

A 70-year-old male was admitted to our hospital due to leukocytosis. On a physical examination, lymphadenopathy extending from the bilateral cervical to supraclavicular regions with moderate hepatomegaly was noted. The laboratory data on admission were as follows: white blood cells (WBC), 248×10^9/L with 0% neutrophils, 1% lymphocytes, 1% monocytes, 0% eosinophils, 0% basophils and 98% atypical lymphocytes, which were medium-sized with pale cytoplasm and prominent nucleoli (Fig. 1A); red blood cells (RBC), 4110×10^9/L; hemoglobin (Hb), 12.4 g/dl; and platelets (Plt), 171×10^9/L. Blood biochemistry was normal, except for elevated levels of lactate dehydrogenase and hepatobiliary enzymes. Bone marrow aspirate smears showed marked proliferation of atypical lymphocytes with a similar morphology to that of the peripheral blood cells. Using a cytogenetic analysis, six of six metaphases examined were 46, XY. A flow cytometric analysis showed that the atypical lymphocytes were positive for CD2, CD4, CD5 and CD7. A *BCR-ABL* FISH analysis showed no *BCR-ABL* signals, although 79 of 100 bone marrow cells exhibited atypical signals (*ABL1*: three copies and *BCR*: two copies in each cell) (Fig. 1B). The three *ABL1* signals indicated either simple amplification of the *ABL1* gene or the presence of *ABL1* rearrangement. In order to examine these two possibilities, the 5′-terminal sequence of the *ABL1* gene was analyzed using the 5′ RACE PCR method (SMARTer

* Correspondence to: Department of Hematology/Oncology, Tokai University School of Medicine, 143 Shimokasuya, Isehara, Kanagawa, Japan.
Tel.: +81 463 93 1121; fax: +81 463 92 4511.
E-mail address: andok@keyaki.cc.u-tokai.ac.jp (K. Ando).

http://dx.doi.org/10.1016/j.lrr.2014.06.004

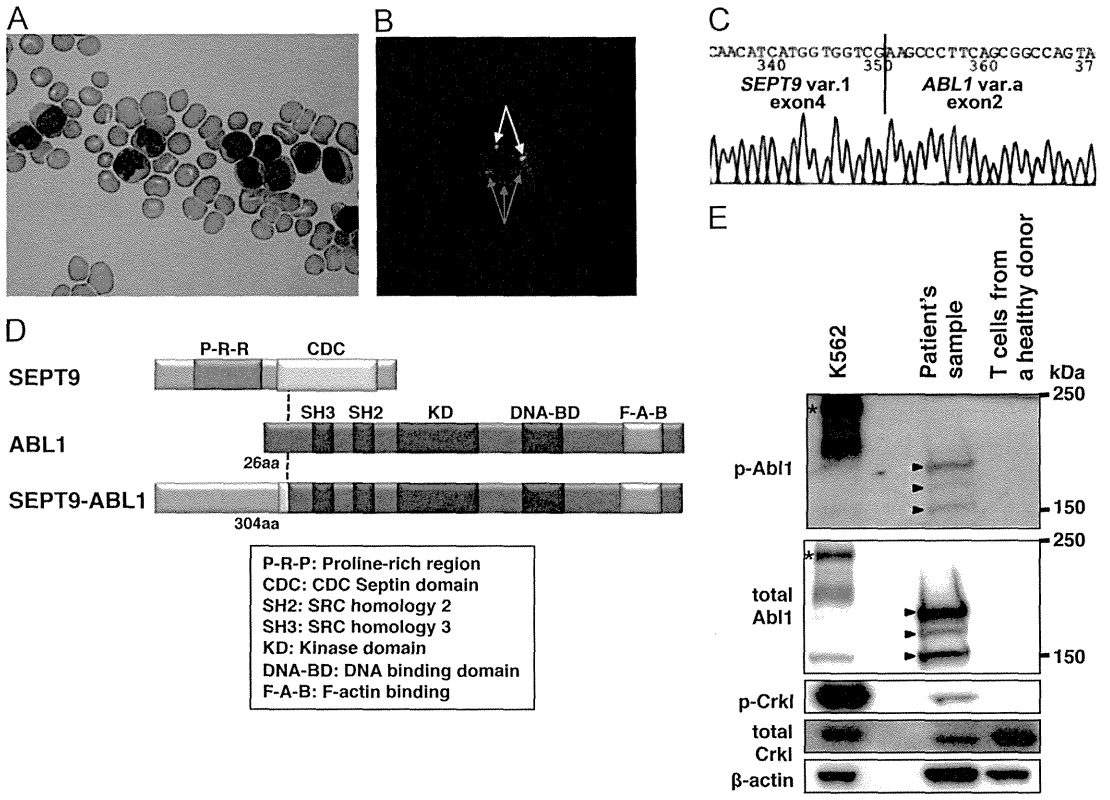

Fig. 1. Clinical and molecular characteristics of T-PLL harboring the *SEPT9-ABL1* fusion gene. (A) Cytology of the leukemic cells in the peripheral blood at diagnosis. The smear underwent Wright–Giemsa staining. (B) A FISH analysis of the bone marrow cells using the *BCR-ABL1* probe. The red signals show three *ABL1* signals, including one normal and two split signals (indicated by the lower arrows), while the green signals show normal biallelic *BCR* signals (indicated by the upper arrows). No *BCR-ABL1* fusion signals were detected. (C) Identification of *SEPT9-ABL1* fusion in the T-PLL cells. The PCR products of 5′ RACE PCR using the ABL1 reverse primer were cloned into a cloning vector. Sequencing of the PCR products showed a fusion of exon 4 of *SEPT9* transcript variant 1 (GenBank accession number: NM_001113491.1) to exon 2 of *ABL1* transcript variant a (GenBank accession number: NM_005157.4). (D) The presumed structure of the SEPT9-ABL1 fusion product. (E) The phosphorylation of SEPT9-ABL1 and the downstream target CRKL in the T-PLL cells obtained from the patient. K562 cells and T-cells derived from a healthy donor were used as positive and negative controls for ABL1 fusion. Anti-ABL1 and anti-phosphorylated-ABL1 antibodies detected three SEPT9-ABL1 bands corresponding to 180, 170 and 150 KDa in the patient (arrowheads), as well as 210 KDa BCR-ABL1 in the K562 cells (asterisks), demonstrating the expression and phosphorylation of SEPT9-ABL1. CRKL was phosphorylated only in the cells harboring ABL1 fusion. The anti-phospho-Abl (Tyr412), anti-Abl, anti-phospho-Crkl (Tyr207) and anti-Crkl antibodies were purchased from Cell Signaling, and anti-β-actin was purchased from Sigma-Aldrich.

RACE cDNA Amplification Kit, Takara Bio, Shiga, Japan), according to the manufacturer's protocol. Sequencing of the PCR products demonstrated the fusion of exon 4 of *SEPT9* to exon 2 of *ABL1* (Fig. 1C), suggesting that the *SEPT9-ABL1* fusion gene had the same breakpoint in *ABL1* as that seen in *BCR-ABL1*. The presumed structure of the SEPT9-ABL1 fusion product is shown in Fig. 1D. A Western blot analysis revealed the expression and phosphorylation of SEPT9-ABL1, in addition to the phosphorylation of a downstream target CRKL, in the T-PLL cells obtained from the patient (Fig. 1E). Taking into account the patient's clinical, morphological, immunophenotypic and molecular features, he was diagnosed with T-PLL harboring *SEPT9-ABL1*. This is the first report of a novel *SEPT9-ABL1* fusion gene in a patient with malignancy, as well as T-PLL harboring *ABL1* fusion.

The patient received multiagent chemotherapy using cyclophosphamide, daunorubicin, vincristine, predonisolone and L-asparaginase, and high dose MTX/Ara-C, as well as the single-agent administration of nelarabine, hydroxyurea and tyrosine kinase inhibitors (TKIs) (imatinib and dasatinib). The conventional chemotherapies and cytotoxic agents effectively reduced the WBC count, however, TKIs were unable to do so. He finally died on day 223 after diagnosis (Fig. 2A). An autopsy was performed, and a macroscopic examination showed generalized lymphadenopathy with an enlarged lung, liver, spleen and kidney, while a microscopic examination disclosed leukemic cell infiltration throughout multiple organs (Fig. 2B). These findings suggested the occurrence of multiple organ failure due to a progression of leukemia which eventually caused the patient's death.

3. Discussion

ABL1 is a well-known oncogene that is often associated with the formation of fusion genes, such as *BCR-ABL1*, in human leukemia. The wild-type ABL1 product transduces diverse extracellular signals to protein networks that control proliferation, survival, migration and invasion [4]. Additionally, ABL1 modulates development and cytoskeletal remodeling processes in T-cells. To date, nine genes, including *BCR*, have been shown to fuse to *ABL1* [5]. These genes are divided into two groups according to their structure: one group has a breakpoint in exon 2 including the Src Homology (SH) 2 and SH3 domains in the fusion products and is found in various kinds of leukemia, while the other has a breakpoint in exon 4 excluding these domains and is primarily found in patients with B-lymphoblastic leukemia (B-ALL). Both groups share the C-terminus structure, including the SH1 tyrosine kinase domain. The N-terminal of the fusion proteins usually includes a coiled-coil or helix-loop-helix domain from the partner protein, which induces the oligomerization of the proteins, thus resulting in tyrosine kinase activation, cytoskeletal localization and neoplastic transformation [5].

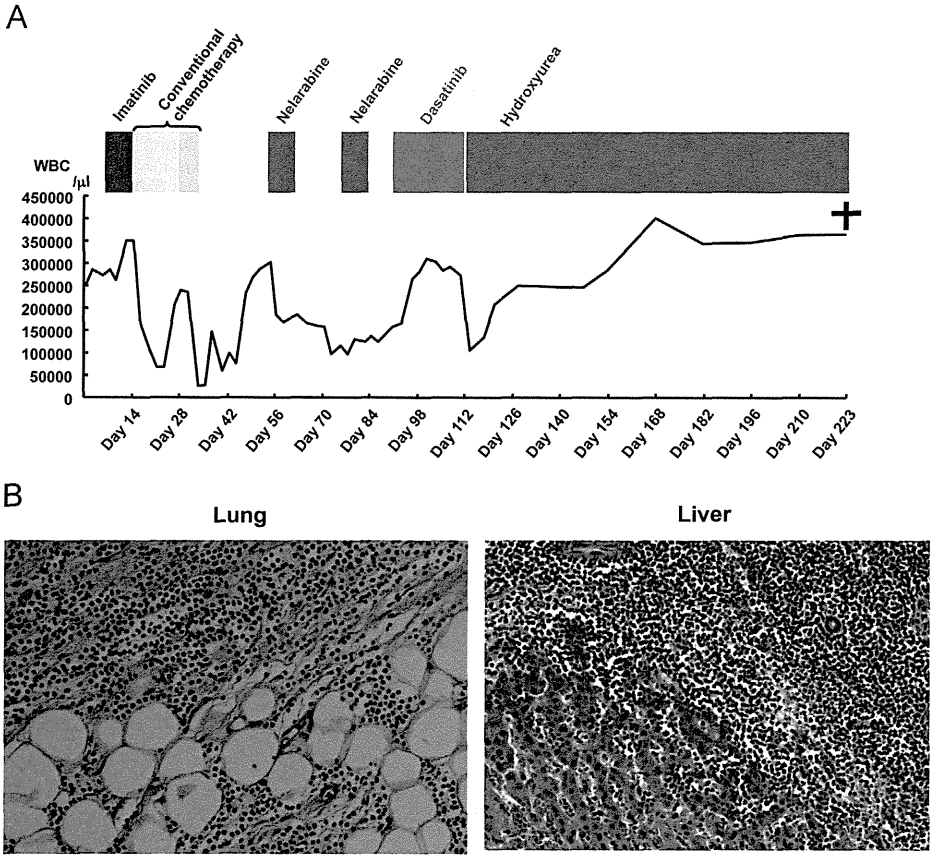

Fig. 2. The refractory clinical course of the patient. (A) The transitional changes in the WBC count in the present case. The administration of imatinib and dasatinib did not reduce the WBC count. (B) The histopathologic examination of the autopsy specimen stained with hematoxylin and eosin showed infiltration of T-PLL cells into the lungs and liver.

Septin proteins belong to a family of proteins that is highly conserved in eukaryotes [6]. These proteins are GTP-binding proteins that form hetero-oligomeric complexes. There are 13 septin genes in humans [6]. The *SEPT9* gene exists at chromosomal location 17q25 and exhibits a ubiquitous expression. SEPT9 plays a role in many cellular mechanisms, such as actin dynamics, axon growth, determination of the cell shape, chromosome segregation, cytokinesis, dendrite formation, DNA repair, membrane trafficking, microtubule regulation and T-cell motility [6]. Furthermore, SEPT9 is deeply associated with the development of various cancers (breast, colon, head, ovarian, neck, leukemia, lymphoma) [6]. In particular, it has been shown that *SEPT9* is a putative proto-oncogene involved in T-cell lymphomagenesis in mice [7].

In patients with hematological malignancies, *MLL* (*KMT2A*)-septin fusion has been repeatedly identified in cells exhibiting myeloid neoplasia in both children and adults. Five different septin genes (*SEPT2*, *SEPT5*, *SEPT6*, *SEPT9* and *SEPT11*) have been identified to be MLL fusion partners [8]. The C-terminal coiled-coil region of septin proteins is preserved in all MLL-septin fusion products, thus indicating that this region contributes to protein–protein interactions and ultimately oncogenesis. In contrast, the N-terminal of SEPT9 is fused to ABL1 in the SEPT9-ABL1 fusion product. It includes the Pro-rich region, which is necessary for binding with SH 3 regions [9]. Because the SH3 domain of ABL1 is preserved in SEPT9-ABL1, this Pro-rich region may contribute to an enhanced chimeric ABL1 kinase potential by promoting interaction with ABL1 SH3 regions, thereby synergistically inducing leukemogenesis.

Regarding the effectiveness of TKIs, some, but not all, patients carrying the *NUP214-ABL1* or *ETV6-ABL1* fusion gene respond to such therapy [5]. A recent report showed that B-ALL with *SNX2-ABL1* responds poorly to dasatinib but partially to imatinib [10,11]. In the present case, SEPT9-ABL1 exhibited a strong resistance to both imatinib and dasatinib. We confirmed that there were no point mutations in the *SEPT9-ABL1* fusion gene. These findings indicate that the TKI response in patients with hematological malignancies associated with various ABL1 fusion products is dependent on the ABL1-partner genes. Further examinations, including conformational analyses of ABL1 fusion products, such as SEPT9-ABL1, and genetic alteration screening of ABL1 fusion-expressing cells, will provide clues uncovering the mechanisms for determining sensitivity to TKI therapy in patients with hematological malignancies harboring *ABL1* fusion products.

Authorship

R.S. performed the experiments, analyzed the data and prepared the manuscript; Hir.M. designed the experiments, performed the experiments, analyzed the data and prepared the manuscript; Hid.K., K.T., Y.O. and Hir.K. analyzed the data; Hid.M. performed the experiments and analyzed the data; K.A. designed the experiments, analyzed the data and prepared the manuscript.

Conflict of interest disclosure

The authors declare no competing financial interests.

References

[1] Matutes E, Brito-Babapulle V, Swansbury J, Ellis J, Morilla R, Dearden C, et al. Clinical and laboratory features of 78 cases of T-prolymphocytic leukemia. Blood 1991;78(12):3269–74.

[2] Hoyer JD, Ross CW, Li CY, Witzig TE, Gascoyne RD, Dewald GW, et al. True T-cell chronic lymphocytic leukemia: a morphologic and immunophenotypic study of 25 cases. Blood 1995;86(3):1163–9.
[3] Dearden CE. T-cell prolymphocytic leukemia. Med Oncol 2006;23(1): 17–22.
[4] Greuber EK, Smith-Pearson P, Wang J, Pendergast AM. Role of ABL family kinases in cancer: from leukaemia to solid tumours. Nat Rev Cancer 2013;13 (8):559–71.
[5] De Braekeleer E, Douet-Guilbert N, Rowe D, Bown N, Morel F, Berthou C, et al. ABL1 fusion genes in hematological malignancies: a review. Eur J Haematol 2011;86(5):361–71.
[6] Mostowy S, Cossart P. Septins: the fourth component of the cytoskeleton. Nat Rev Mol Cell Biol 2012;13(3):183–94.
[7] Connolly D, Abdesselam I, Verdier-Pinard P, Montagna C. Septin roles in tumorigenesis. Biol Chem 2011;392(8–9):725–38.
[8] Cerveira N, Bizarro S, Teixeira MR. MLL-SEPTIN gene fusions in hematological malignancies. Biol Chem 2011;392(8–9):713–24.
[9] Boggon TJ, Eck MJ. Structure and regulation of Src family kinases. Oncogene 2004;23(48):7918–27.
[10] Masuzawa A, Kiyotani C, Osumi T, Shioda Y, Iijima K, Tomita O, et al. Poor responses to tyrosine kinase inhibitors in a child with precursor B-cell acute lymphoblastic leukemia with SNX2-ABL1 chimeric transcript. Eur J Haematol 2014;92(3):263–7.
[11] Tomita O, Iijima K, Ishibashi T, Osumi T, Kobayashi K, Okita H, et al. Sensitivity of SNX2-ABL1 toward tyrosine kinase inhibitors distinct from that of BCR-ABL1. Leuk Res 2014;38(3):361–70.

OPEN ACCESS Freely available online

PLOS ONE

Establishment of a Humanized APL Model via the Transplantation of *PML-RARA*-Transduced Human Common Myeloid Progenitors into Immunodeficient Mice

Hiromichi Matsushita[1,2,3]*, Takashi Yahata[1,2,4], Yin Sheng[1], Yoshihiko Nakamura[1], Yukari Muguruma[1], Hideyuki Matsuzawa[1,5], Masayuki Tanaka[5], Hideki Hayashi[5], Tadayuki Sato[5], Anar Damdinsuren[3], Makoto Onizuka[6], Mamoru Ito[7], Hayato Miyachi[3], Pier Paolo Pandolfi[8], Kiyoshi Ando[1,2,6]*

1 Research Center for Cancer Stem Cell, Tokai University School of Medicine, Isehara, Kanagawa, Japan, **2** Medical Research Institute, Tokai University, Isehara, Kanagawa, Japan, **3** Department of Laboratory Medicine, Tokai University School of Medicine, Isehara, Kanagawa, Japan, **4** Department of Cell Transplantation, Tokai University School of Medicine, Isehara, Kanagawa, Japan, **5** Support Center for Medical Research and Education, Tokai University, Isehara, Kanagawa, Japan, **6** Division of Hematology and Oncology, Department of Internal Medicine, Tokai University School of Medicine, Isehara, Kanagawa, Japan, **7** Central Institute for Experimental Animals, Kawasaki, Kanagawa, Japan, **8** Cancer Research Institute, Beth Israel Deaconess Cancer Center, Departments of Medicine and Pathology, Beth Israel Deaconess Medical Center, Harvard Medical School, Boston, Massachusetts, United States of America

Abstract

Recent advances in cancer biology have revealed that many malignancies possess a hierarchal system, and leukemic stem cells (LSC) or leukemia-initiating cells (LIC) appear to be obligatory for disease progression. Acute promyelocytic leukemia (APL), a subtype of acute myeloid leukemia characterized by the formation of a PML-RARα fusion protein, leads to the accumulation of abnormal promyelocytes. In order to understand the precise mechanisms involved in human APL leukemogenesis, we established a humanized *in vivo* APL model involving retroviral transduction of *PML-RARA* into $CD34^+$ hematopoietic cells from human cord blood and transplantation of these cells into immunodeficient mice. The leukemia well recapitulated human APL, consisting of leukemic cells with abundant azurophilic abnormal granules in the cytoplasm, which expressed CD13, CD33 and CD117, but not HLA-DR and CD34, were clustered in the same category as human APL samples in the gene expression analysis, and demonstrated sensitivity to ATRA. As seen in human APL, the induced APL cells showed a low transplantation efficiency in the secondary recipients, which was also exhibited in the transplantations that were carried out using the sorted $CD34^-$ fraction. In order to analyze the mechanisms underlying APL initiation and development, fractionated human cord blood was transduced with *PML-RARA*. Common myeloid progenitors (CMP) from $CD34^+/CD38^+$ cells developed APL. These findings demonstrate that CMP are a target fraction for *PML-RARA* in APL, whereas the resultant $CD34^-$ APL cells may share the ability to maintain the tumor.

Citation: Matsushita H, Yahata T, Sheng Y, Nakamura Y, Muguruma Y, et al. (2014) Establishment of a Humanized APL Model via the Transplantation of *PML-RARA*-Transduced Human Common Myeloid Progenitors into Immunodeficient Mice. PLoS ONE 9(11): e111082. doi:10.1371/journal.pone.0111082

Editor: Marina Konopleva, University of Texas M.D. Anderson Cancer Center, United States of America

Received February 27, 2014; **Accepted** September 24, 2014; **Published** November 4, 2014

Funding: Hiromichi Matsushita received funding from a Grant-in-Aid for Scientific Research from The Ministry of Education, Culture, Sports, Science and Technology of Japan (#24591411, URL http://www.jsps.go.jp/english/e-grants/), Tokai University School of Medicine Project Research (http://www.med.u-tokai.ac.jp/web/international/about_us/message_from_the_dean.html), and the Takeda Science Foundation (http://www.takeda-sci.or.jp/index.html). Kiyoshi Ando received support from a Grant-in-Aid for Scientific Research from The Ministry of Education, Culture, Sports, Science and Technology of Japan (#24390248). The funders had no role in study design, data collection and analysis, decision to publish, or preparation of the manuscript.

Competing Interests: The authors have declared that no competing interests exist.

* Email: hmatsu@is.ic.cc.u-tokai.ac.jp (H. Matsushita); andok@keyaki.cc.u-tokai.ac.jp (KA)

Introduction

Acute myeloid leukemia (AML) constitutes a heterogeneous group of tumors in myeloid lineage cells characterized by the proliferation and accumulation of immature myeloblasts [1]. Recent advances in cancer biology have revealed that various genetic events result in the blockage of differentiation with subsequent uncontrolled cellular proliferation. In addition, *in vivo* analyses using a xenograft model with immunodeficient mice have shown that a very immature subset of AML cells called leukemic stem cells (LSC), which are typically characterized as $CD34^+/CD38^-$ cells, as observed in normal hematopoietic stem cells (HSCs), have been shown to slowly undergo cell division to both yield progenitor cells and sustain the LSC population, thus resulting in the maintenance of the tumor [2–6]. More recently, several reports have shown that $CD34^+/CD38^+$ hematopoietic progenitors are able to acquire the ability to maintain populations of LSC or leukemia-initiating cells (LIC) [7]. It is therefore possible that the phenotypes of LIC differ among the subtypes of AML.

Acute promyelocytic leukemia (APL) is a subset of AML defined by the formation of a chimeric gene, promyelocytic leukemia-retinoic acid receptor α (*PML-RARA*) [8]. It is characterized by the accumulation of abnormal promyelocytes with abundant large azurophilic granules, suggesting that APL cells undergo maturation arrest in the later steps of myeloid differentiation. The typical pattern of cellular surface markers of APL is positive for CD13,

CD33 and CD117, and negative for CD34, which is usually presumed to indicate cellular immaturity, and HLA-DR [9]. It is very difficult to engraft primary APL samples in immunodeficient mice. They did not become engrafted into the NOD/SCID mice to any degree [3]. In NOD/Shi-SCID/IL-2Rγ^{null} (NOG) mice, which are more profoundly immunocompromised than NOD/SCID mice [10,11], six out of eight APL samples were not engrafted or only very little engrafted [12]. It is therefore possible that the mechanisms underlying the development of APL differ from those involved in the pathogenesis of AML uncovered to date. Elucidating the pathogenesis of APL is important for improving the treatment of APL patients, and will provide clues to understand the development of other subtypes of AML.

In vivo analyses using transgenic APL mice models with *PML-RARA* have revealed that a population of committed myeloid progenitor cells (CD34$^+$, c-kit$^+$, FcγRIII/II$^+$, Gr1^{int}) was identified as the APL-LIC [13,14]. However, the cellular surface antigens and the gene expression pattern in humans are different from those in mice. In particularly, in transgenic systems, murine APL developed after a long latent period through a myelodysplastic/proliferative phase, which does not usually precede human APL [15–18]. There have been no *in vivo* models for exploring leukemogenesis of human APL to date; largely because human primary APL cells are difficult to engraft as a xenograft [3,12]. *PML-RARA*-retrovirally transduced human CD34$^+$ cells from cord blood have therefore only been evaluated *in vitro* [19].

Therefore, the aim of this study was to establish a humanized xenograft APL model using the retroviral transduction of *PML-RARA* into human CD34$^+$ cells and NOG mice in order to investigate the mechanisms of APL leukemogenesis, such as that involving disease initiation and maintenance in the model.

Materials and Methods

Fractionation of human hematopoietic cells from cord blood

Cord blood (CB) and patients' APL samples were obtained after written informed consent was provided in accordance with the Declaration of Helsinki and with approval from the Tokai University Committee on Clinical Investigation (Permit number: #12I-46 and #12I-49). CD34 positive and negative specimens were primarily prepared using the CD34 Progenitor Cell Isolation Kit (Miltenyi Biotec, Bergisch Gladbach, Germany). CD34$^+$ cells were then purified again using anti-human CD34 mAbs (Beckman Coulter, Brea, CA), in combination with or without an anti-CD38 antibody (BD, Franklin Lakes, NJ), with a FACS vantage instrument (BD). CD34$^-$/CD33$^+$ cells were also purified again using anti-human CD34 and CD33 mAbs (Beckman Coulter) and the FACS vantage instrument. The preparation of common myeloid progenitors (CMP), granulocyte-monocytic progenitors (GMP) and megakaryocyte-erythrocyte progenitors (MEP) was performed using an anti-CD123 antibody (BD) and anti-CD45RA (Biolegend, San Diego, CA) antibody, according to a previous report [20].

Retrovirus transduction of *PML-RARA* into human hematopoietic cells

The MIGR1 retroviral vector [21] or MIGR1-*PML-RARA* (bcr3/short form) [22] in combination with the vesicular stomatitis virus-G protein (VSV-G) envelope vector (pCMV-VSV-G) was transiently transfected into PLAT-gp cells using the Fugene 6 transfection reagent (Roche Diagnostics, Basel, Switzerland). The culture supernatant was concentrated 100 to 200 times by ultracentrifugation. After overnight culture of the fractionated cells in StemPro-34 (Life Technologies, Carlsbad, CA) with TPO, SCF, and FLT3 ligand (50 ng/ml each), they were incubated with the concentrated supernatant on retronectin-coated plates (Takara-Bio, Otsu, Japan). Retroviral transduction was performed twice, and then transplantation was performed the next day.

Colony-forming unit-cells assay

PML-RARA transduced cells were sorted by their EGFP, CD34 and CD38 expression by FACS vantage 48 h after infection. The colony-forming unit-cells (CFU-C) assay was performed as described previously [23]. The fluorescent images were captured using a HS All-in-One Fluorescence Microscope Biorevo 9000 (Keyence Corporation, Osaka, Japan) and were analyzed by the BZ II software program (Keyence Corporation).

RNA extraction and RT-PCR

Total RNA was isolated using the RNeasy micro kit (Qiagen, Hilden, Germany) or Isogen (Nippon gene, Tokyo, Japan), and the reverse-transcribed cDNA was amplified by qualitative PCR. The qualitative-PCR analysis was performed by SRL Inc. (Hachioji, Tokyo, Japan). The sequences of PCR primers and probes were shown in **Table S1**.

Transplantation, serial transplantation and ATRA treatment

Nine- to 20-week-old NOD/Shi-scid, IL-2Rγc^{null} (NOG) mice [10,11] were irradiated with 220 cGy of X-rays. On the following day, the whole infected cells or primary AML cells were intravenously injected. The EGFP-positive cells in the peripheral blood were monitored. The mice with induced APL were defined as those bearing more than 0.1% EGFP$^+$ cells which dominantly expressed CD33 (more than 70%) in their bone marrow at four months after transplantation. In the initial analysis, the occurrence of APL was confirmed by the morphological observations using cytospin slides after EGFP sorting. For serial transplantation, bone marrow cells were obtained from recipient mice, and the sorted EGFP-positive cells were injected intravenously or intramedullary into the irradiated mice [24]. The engrafted mice were treated intraperitoneally with 1.5 μg/g of body weight/day of all-*trans* retinoic acid (ATRA, Sigma) for 21 days [25], and were then sacrificed to collect the EGFP-positive cells in the bone marrow by sorting. All the experiments using animals were approved by the animal care committee of Tokai University (Permit number: #132028).

Flow cytometric analysis

The cells were stained with APC-conjugated anti-human CD45, CD33, CD34, HLA-DR (Beckman Coulter), CD13, and CD117 (BD) mAbs. They were subjected to flow cytometry using a FACSCalibur instrument (BD) and the CellQuest software program (BD).

Cell preparation, Wright-Giemsa staining and immunofluorescence microscopy

Cytospin slides were prepared using a Cytospin 4 Cytocentrifuge (Thermo Scientific, Waltham, MA) at 500 rounds per minute for 5 min. To observe the cellular morphology, Wright-Giemsa staining was performed. For the immunofluorescent study, cells were seeded onto poly-L-lysine coated slides and fixed with ice cold 70% ethanol for 15 min. After permeabilization with 0.2% Triton X-100 for 20 min, the slides were treated with PBS containing 5% normal goat serum for 1 hour to block the nonspecific binding of antibodies. The anti-PML antibody (Merck

Millipore, Billerica, MA) was applied overnight at 4°C. Cells were counterstained with DAPI. Images were captured with an LSM510 META confocal microscope (Carl Zeiss, Oberkochen, Germany) and processed using Adobe Photoshop 7.0 (Adobe Systems, San Jose, CA).

Southern blot analysis

Genomic DNA was extracted from the cells using a DNeasy kit (Qiagen). Ten micrograms of the DNA were electrophoresed and transferred to nylon membranes (Hybond-N+, GE Healthcare, Fairfield, CT). The DNA was then crosslinked to the membrane by ultraviolet light. The EGFP probe was prepared from MIGR1 vector by cutting it using NcoI and SalI, and was labeled with ^{32}P-dCTP using the Rediprime II DNA Labelling System (GE Healthcare). The membrane was hybridized with the probe in Rapid-hyb buffer (GE Healthcare), and was analyzed by a Phosphoimager (LAS1000, Fuji Film, Tokyo, Japan).

Microarray

Total RNA was labeled and hybridized to Affymetrix Human Genome U133 Plus 2.0 Array GeneChip microarrays (Affymetrix, Santa Clara, CA) using the manufacturer's protocols. The results were deposited in the Gene Expression Omnibus (GEO; http://www.ncbi.nlm.nih.gov/geo/; accession no. GSE49344). The microarray data from normal human promyelocytes and clinical samples bearing AML, including APL, were obtained from the deposited data on the GEO (GSE12662). The APL-specific expressed genes have been described in detail in a previous study [26]. The probe set data were generated using standard normalization algorithms included in the Affymetrix Microarray Suite software program, v.5 (MAS5.0). The clustering analysis was performed by the Gene spring GX software program, version 11 (Agilent technology, Santa Clara, CA).

To identify the genes that are differentially expressed in a specific cellular subset, all probe sets with fewer than 10% present calls in both groups and a coefficient of variation <0.5 across all samples were eliminated prior to the subsequent analysis; (i) The genes differently expressed in the induced APL cases among the AML cases were defined as genes whose expression change (upregulation or downregulation) was ≥2.0 fold in comparison to those in AML other than APL, (ii) The genes associated with immaturity in the induced APL cases were expressed at significantly higher levels in CD34$^+$ cells than the other normal cells (FDR <0.05, fold-change >2.0 upregulated), and were also expressed in the induced APL cells at similar levels (induced APL: CD34$^+$ ≥1:1), and moreover, these genes were expressed at higher levels in promyelocytes (induced APL: Pros ≥2:1). (iii) The genes upregulated during promyelocyte differentiation were expressed at significantly higher levels in promyelocytes than in the other normal cells (FDR <0.05, fold-change >2.0 upregulated), and were expressed at lower levels in the induced APL (induced APL: Pros ≤1:2), (iv) The genes induced by *PML-RARA* were expressed at higher levels in the induced APL than in all the normal cells (induced APL: normal ≥2:1), and were not expressed in any normal cells (more than 75% absent calls, as summarized by the MAS5.0). Statistical significance was assessed by the unpaired unequal variance Welch test (P<0.05), and correction for multiple testing was performed by the Benjamini and Hochberg False Discovery Rate (FDR), using a cutoff of 0.05.

The gene set specific for induced APL was defined to fulfill one or more of the above criteria (ii) to (iv) in the gene set identified in (i).

The integration site analysis of *PML-RARA* using linear amplification-mediated PCR

To identify the genomic-proviral junction sequence, linear amplification-mediated polymerase chain reaction (LAM-PCR) was performed as described previously, with minor modifications [27,28]. In brief, genomic DNA from bone marrow cells was first digested with Tsp509I. A linear amplification of target DNA in the digested genome was performed by repeated primer extension using a vector-specific 5′-biotinylated primer, LTR1.5, and Taq polymerase. After selection with Dynabeads MyOne Streptavidin C1 (Life Technologies), a double-stranded asymmetrical linker cassette was ligated to the Tsp509I-digested site using T4 DNA Ligase. The DNA products were then amplified by PCR using a vector-specific primer, LTR3, and linker cassette primer, LC1. The nested PCR was performed using internal primers LTR5 and LC2. The final products were sequenced after cloning them into the TOPO TA cloning vector (Life Technologies). The primer sequences are shown in **Table S1**.

Statistical analyses

The Kaplan-Meier method was used to estimate the leukemia-free survival (LFS) of mice. Log-rank p values were used for comparisons of the LFS among three subgroups. The analyses were conducted using the GraphPad Prism software package (GraphPad Software, La Jolla, CA). The other statistical analyses were performed using the Mann-Whitney U Test with the IBM SPSS Statistics software program (New York, NY). Values of p< 0.05 were considered to be statistically significant.

Results

Functions of PML-RARα in human CD34 cells *in vitro*

To examine the functions of PML-RARα *in vitro*, a MIGR1-*PML-RARA* or MIGR1 control vector was retrovirally infected into human CD34$^+$ cells from cord blood. The transduction efficiency evaluated by EGFP positivity was 0.5% to 18.6% (n = 10, median: 5.7%) and 2.1% to 19.7% (n = 25, median: 6.8%), respectively. The expression of *PML-RARA* in these cells was confirmed by RT-PCR (**Figure S1**). The induction of *PML-RARA* in CD34$^+$ cells disrupted PML nuclear bodies by interacting with wild-type PML via the PML portion of the chimeric transcript, and the distribution of PML in the nucleus was altered to show a microspeckled pattern in these cells [29–31] (**Figure 1A**). Additionally, the induction of *PML-RARA* reduced all the colony formation capacity (**Figure 1B**). The *PML-RARA* expression was confirmed in these colonies by EGFP fluorescence (**Figure S1 and S2**) and RT-PCR, although the expression levels were 37 times lower compared to those in the CD34$^+$ cells 48 hours after *PML-RARA* transduction (**Figure S3**). Regarding the content of colonies, MIGR1-infected CD34$^+$ cells mainly generated the erythroid lineage-containing colonies, such as CFU-mix and BFU-E, whereas more than half of the colonies from the CD34$^+$ cells with *PML-RARA* were of the myeloid lineage, like CFU-GM (**Figures 1C**). These data demonstrate that *PML-RARA* induces the myeloid commitment of human CD34$^+$ cells.

Establishment of a humanized *in vivo* APL model

The cells transduced with *PML-RARA* or the MIGR1 control vector were then transplanted into NOG mice. The EGFP$^+$ cells survived and proliferated three to four months after transplantation only in the NOG mice transplanted with *PML-RARA*-, not control vector at all, infected human CD34$^+$ cells. The median proportion of EGFP$^+$/CD45$^+$ cells in the bone marrow obtained from the transplanted mice was 23.7% (0.95% to 96.5%, n = 24)

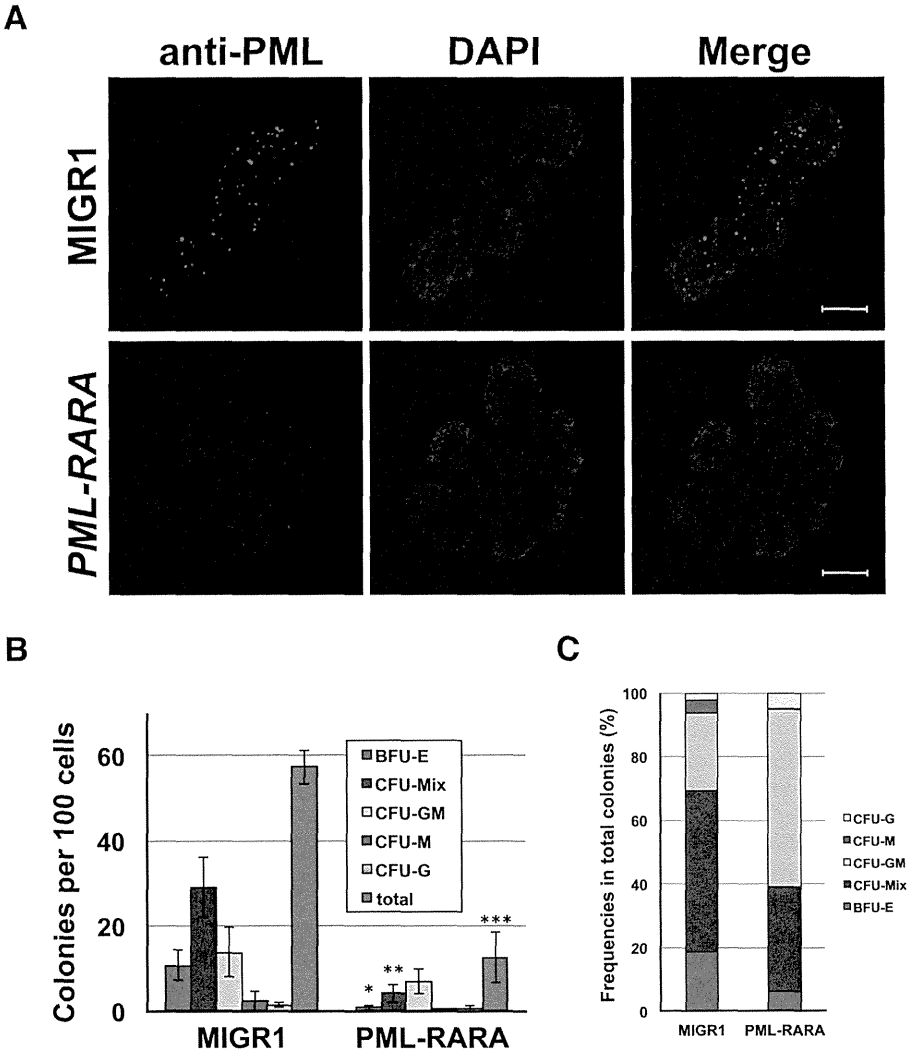

Figure 1. The function of *PML-RARA* in human CD34$^+$ cells *in vitro*. (**A**) The results of an immunofluorescent analysis of PML distribution in human CD34$^+$ cells transduced with *PML-RARA*. The images were captured with an LSM510 META confocal microscope (Carl Zeiss). The bars indicate 10 μm. (**B**) The colony-forming assay using *PML-RARA*-transduced CD34$^+$ cells. The cells were sorted by EGFP expression 48 h after infection. Colony formation was evaluated on days 10 to 12 after plating the cells. The average numbers of colonies from three independent experiments are shown. Data represent the means ± SD. The asterisks (*) indicate $p<0.05$. (**C**) The proportion of each kind of colony was calculated from the results of the colony-forming assay shown in (B). The percentages of CFU-GM are higher in *PML-RARA*-infected cells than in control (MIGR1) cells ($p=0.013$).
doi:10.1371/journal.pone.0111082.g001

(**Figure 2A**). The majority of the engrafted EGFP$^+$/human CD45$^+$ cells expressed human CD33 (70.2% to 100%, median 90.6%, n = 24) (**Figure 2B**), thus suggesting that they were of the myeloid lineage. The *PML-RARA* expression was detected only in the EGFP$^+$ fraction and not in the EGFP$^-$ fraction of the sorted human CD45$^+$/CD33$^+$ cells from the NOG mice (**Figure 2C**). The expression levels of *PML-RARA* were decreased about 17-fold in comparison to those in the CD34$^+$ cells 48 hours after *PML-RARA* transduction (**Figure S3**), but the presence of *PML-RARA* in the human myeloid cells, recognized as EGFP$^+$ cells, caused marked accumulation of promyelocytes, in comparison to the control EGFP$^-$ human myeloid cells (52.8% in EGFP$^+$ cells vs 19.4% EGFP$^-$ cells in the 13 paired samples, $p<0.0001$). On the other hand, the proportions of myeloblasts, mature neutrophils and monocytes were decreased (5.2% vs 14.4%, $p=0.010$; 2.5% vs 12.7%, $p=0.005$; 4.0% vs 10.1%, $p=0.016$) (**Figure 2D**). These findings confirmed that the expression of *PML-RARA* induced the myeloid differentiation of human CD34$^+$ cells and blocked them at the promyelocytic stage. Morphologically, the promyelocytes had abundant large azurophilic granules and round nuclei with a high nucleocytoplasmic ratio. Some of them had a number of Auer bodies and looked like Faggot cells, which are the typical morphological features of APL cells, and were not seen in the previous murine models (**Figure 2E**). A Southern blot analysis using an EGFP probe revealed that the EGFP$^+$/CD45$^+$/CD33$^+$ cells oligoclonally proliferated *in vivo* (**Figure 2F**).

The induced APL cells were detected in 24 out of the 34 mice (71%) transplanted with *PML-RARA*-transduced CD34 cells ($p=0.0184$ in comparison to the control). They were detected in all 16 mice when the calculated number of the transplanted EGFP$^+$/CD34$^+$ cells per mouse was more than 3,000 (4,655 to 29,728 cells, median: 11,085 cells) ($p=0.0006$ in comparison to the control). On the other hand, they were only detected in eight out of 18 mice (44%) transplanted with EGFP$^+$/CD34$^+$ cells at a

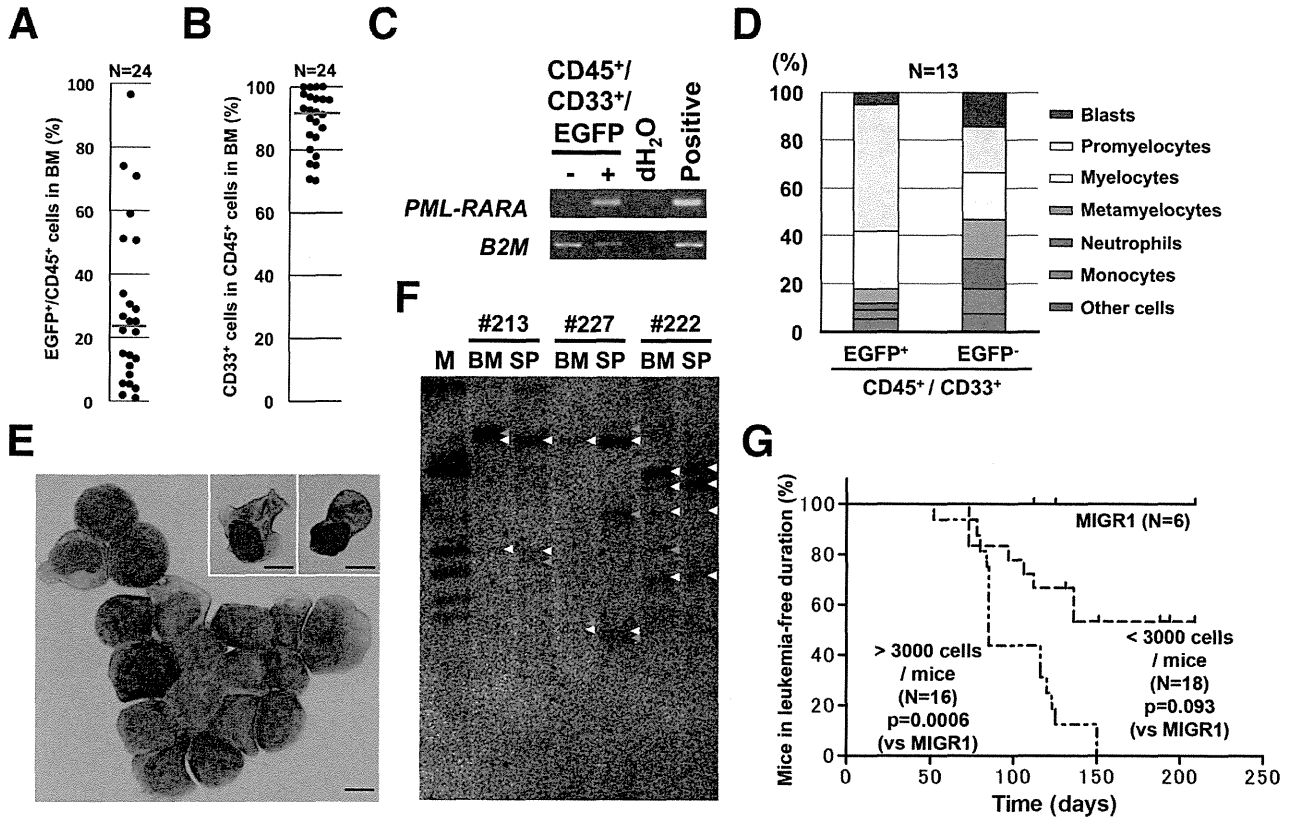

Figure 2. Establishment of humanized APL *in vivo*. (**A**) The proportion of EGFP$^+$/human CD45$^+$ cells in the bone marrow of leukemic NOG mice. Each dot represents a single mouse. The horizontal line represents the median value. (**B**) The proportion of CD33$^+$ cells among the EGFP$^+$/human CD45$^+$ cells in the bone marrow of the leukemic NOG mice. Each dot represents a single mouse. The horizontal line represents the median value. (**C**) The expression of *PML-RARA* in RT-PCR was detected only in the EGFP$^+$ fraction obtained from the engrafted human CD45$^+$/CD33$^+$ cells. The cells were obtained from bone marrow 16 weeks after transplantation. *B2M, beta 2 microglobulin*. The *PML-RARA* expression vector and human CD34$^+$ cells were used as a positive control for the *PML-RARA* and *B2M* analysis, respectively. (**D**) The differential counts of the engrafted CD45$^+$/CD33$^+$/EGFP$^+$ and EGFP$^-$ cells from the mice transplanted with *PML-RARA*-induced human CD34$^+$ cells. They were obtained from bone marrow 16 to 20 weeks after transplantation. The data represent the means. (**E**) A representative photograph of the resulting leukemic cells which morphologically recapitulated APL. Faggot cells were recognized, as seen in the right top corner. The images were captured with a BX41 microscope (Olympus). The bar indicates 10 μm. (**F**) The results of a Southern blot analysis of the genomic DNA from induced APL cells with an EGFP probe. Clonal bands are shown by arrow heads: white, seen in both BM and SP; orange, seen only in BM or SP. BM, bone marrow; SP, spleen. (**G**) The leukemia-free duration in NOG mice transplanted with *PML-RARA*-transduced CD34$^+$ cells.
doi:10.1371/journal.pone.0111082.g002

density of less than 3,000 (480 to 2,660 cells, median: 1,861 cells) ($p = 0.093$ in comparison to the control) (**Figure 2G**). This proportion was not dependent on the number of transplanted EGFP$^+$/CD34$^+$ cells.

These findings demonstrate that a humanized APL model can be successfully established by the transplantation of *PML-RARA*–transduced human CD34 cells into NOG mice.

Characteristics of the induced APL cells obtained from the humanized *in vivo* model

The induced APL cells were positive for human myeloid markers such as CD13, CD33 and CD117, and were negative for CD34 and HLA-DR, as seen in typical human APL [32]. *PML-RARA* did not contribute to the development of lymphocytes. Human CD19$^+$ B-cells in the spleen and human CD4$^+$/CD8$^+$ T-cells in the thymus were negative for EGFP (**Figure 3A**).

To evaluate the gene expression of the induced APL cells, a microarray analysis was performed, and the expression of the 510 APL-specific genes identified in a previous study was compared with that observed in the clinical AML samples [26]. Two clinical APL samples from our patients were simultaneously evaluated and were aligned in the APL category defined in the study, suggesting that our microarray results were comparable with those in the previous study. The induced APL cells from our models were also classified into the APL category when compared to normal promyelocytes and AML samples other than APL (**Figure 3B**).

In common with this previous study [26], the 3,439 probes (3278 genes) differentially expressed in the induced APL and the AML other than APL ((i) in the Materials and Methods) grouped the induced APL and human primary APL together, separately from the other types of AML (**Figure S4**). The gene sets whose expression in the induced APL cases was not dependent on the myeloid differentiation were also filtered by comparison with the data for normal myeloid cells. They included the genes for immaturity expressed in the induced APL (1,782 probes, including 1,720 genes), the genes upregulated in promyelocyte differentiation not in the induced APL (447 probes, including 427 genes) and the genes specifically induced by *PML-RARA* (466 probes, including 429 genes) ((ii), (iii) and (iv) in the Materials and Methods). Each gene set was analyzed using the DAVID website

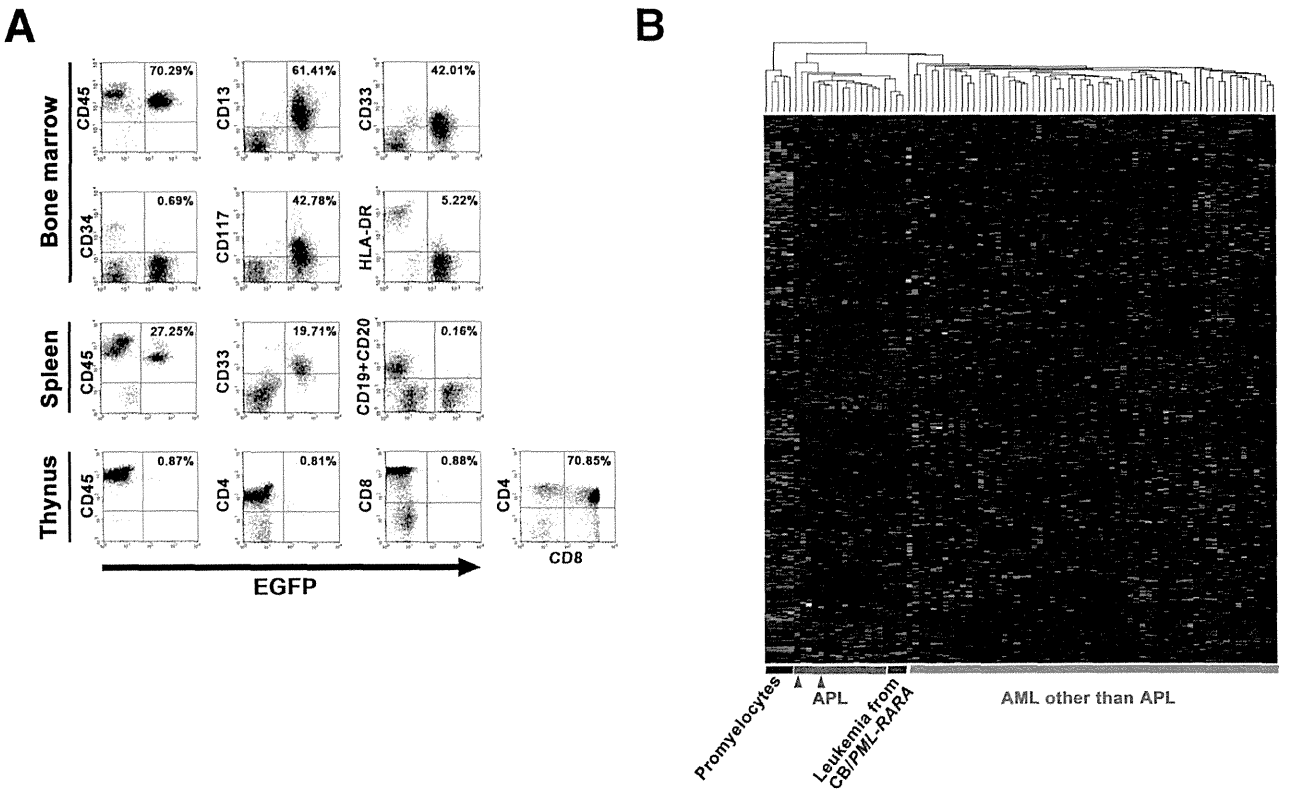

Figure 3. Characteristics of the induced APL *in vivo*. (**A**) The representative expression pattern of cell surface markers in the induced APL cells determined by a flow cytometric analysis. All the scatter plots show the relationships between the EGFP positivity and cell surface marker expression. The whole living cells gated as a propidium iodide-negative fraction in the bone marrow were analyzed. The induced APL cells were recognized as $EGFP^+$ cells. A few murine hematopoietic cells, recognized as a human $CD45^-$ fraction, were detected in this mouse. (**B**) The heat map of the microarray analysis using the 510 APL-specific genes for the comparison of the induced APL cells (purple, n = 3) with APL (red, n = 16), other types of AML (M0, 1, 2 and 4 in FAB classification, green, n = 62) and normal promyelocytes (blue, n = 5) in a previous study [26]. The red triangles (n = 2) for a total 16 APL cases show the clinical APL samples whose microarray data were obtained in this study.
doi:10.1371/journal.pone.0111082.g003

(david.abcc.ncifcrf.gov/). In the induced APL cases, the genes related to N-Glycan, steroid and heparan sulfate biosynthesis, the spliceosome and pyrimidine metabolism were expressed similar to the levels in normal $CD34^+$ cells, and those related to the MAPK signaling pathway were exclusively expressed in comparison to normal myeloid cells, including normal $CD34^+$ cells. On the other hand, the genes related to neurotrophin signaling and the cell cycle, as well as those associated with metabolic processes, such as glycolysis/gluconeogenesis, the pentose phosphate pathway and sphingolipid metabolism were downregulated (**Table S2**), thus suggesting that the induced APL exhibited dysregulated signaling and metabolism as differentiated myeloid cells. Additionally, the gene set composed of 573 probes including 547 genes, which fulfilled one or more above criteria (ii) to (iv) in the gene set identified in (i), clearly separated the normal and malignant promyelocytes, such as those of induced and human primary APL (**Figure S5 and Table S3**), as described in the previous study using primary APL cases [26].

To evaluate the additional genetic events that accompanied the integration of *PML-RARA* in the genome, the insertion sites of *PML-RARA* were analyzed. Some of the integration sites of *PML-RARA* were in the introns or exons of genes (**Table S4**). However, they were neither recurrent nor found in the previous whole genome sequence analysis of the APL patients [33]. These findings suggest that *PML-RARA* was a common key event, but that there were various additional genetic events in these induced APL cells, and this finding was compatible with the previous analysis using human primary APL [33].

The induced APL cells differentiated into mature neutrophils following treatment with all-*trans* retinoic acid (ATRA) *in vitro* (**Figures 4A and 4B**), which was accompanied by alterations in the PML distribution in the nucleus, from a microspeckled to a speckled pattern (**Figure 4C**). Similarly, ATRA induced transient myeloid differentiation *in vivo* (n = 4), as has been seen in APL patients (**Figures 4D and 4E**).

These findings demonstrate that our induced APL cells recapitulate human APL both phenotypically and functionally.

Re-transplantable cellular fraction in the induced APL cells

It is necessary to prove that the resultant induced APL cells possess the reproducibility of APL in the secondary recipients in order to demonstrate their capacity for leukemogenesis. However, previous studies have revealed that primary APL cells exhibit difficultly in engrafting in immunodeficient mice [3,12]. When the induced APL cells were transplanted into the second recipients, they were proven to be re-transplantable intravenously; 500,000 to 1,000,000 leukemic cells, but not 50,000 cells, were required, and the frequency of APL cells in the secondary recipients was low (0.04% to 1.41%, n = 6). The frequency was still low, even though

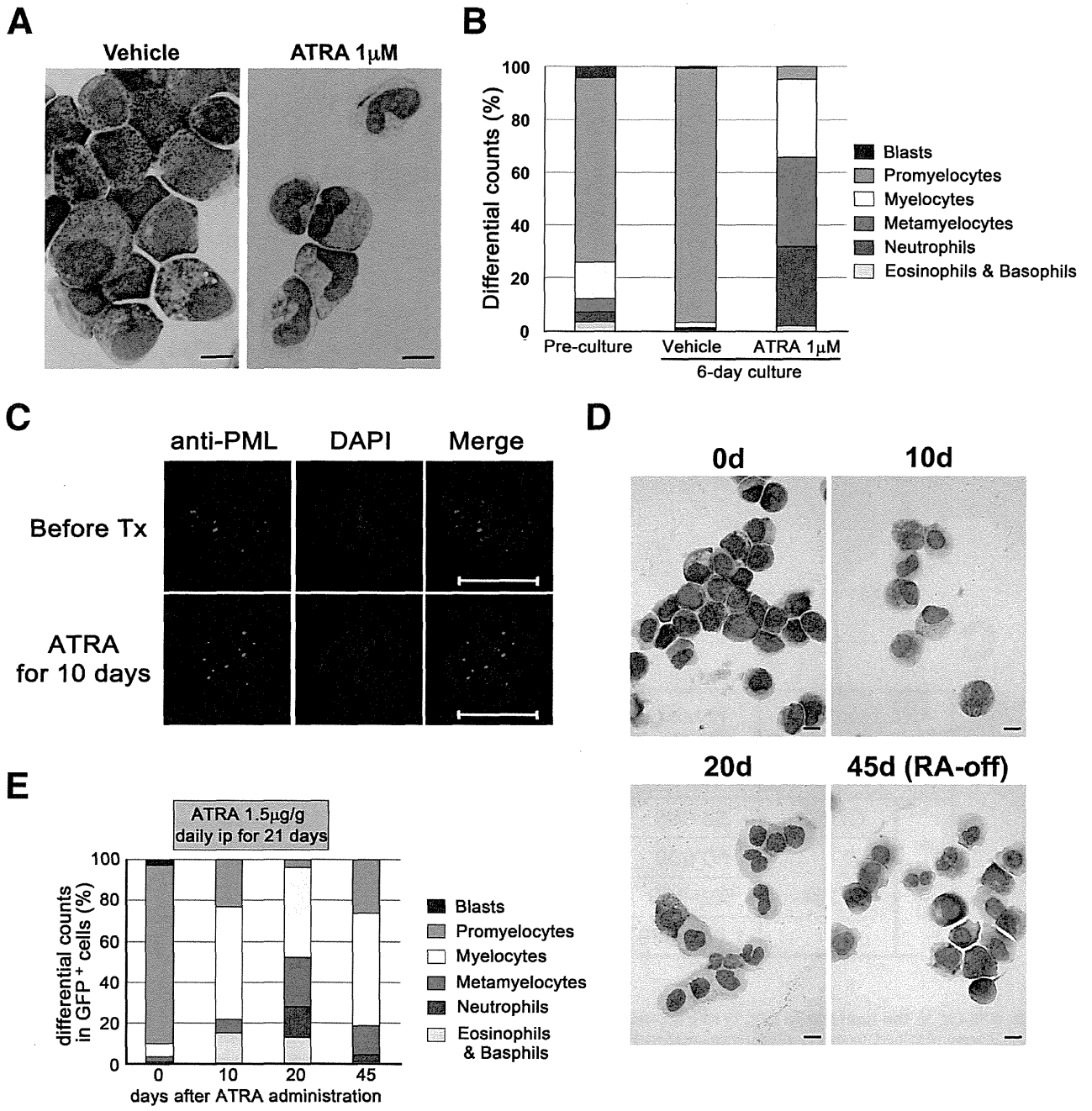

Figure 4. The induction of myeloid differentiation in the APL cells induced by ATRA treatment *in vitro* and *in vivo*. (**A**) Cytospin slides of the induced APL cells cultured with or without 1 μM ATRA for 6 days. The mature neutrophils with Auer rods are seen in the ATRA-treated group. The images were captured with a BX41 microscope (Olympus). The bar indicates 10 μm. (**B**) The differential cellular counts of the induced APL cells cultured with or without ATRA. The average leukocyte differentiation in three independent experiments is shown. (**C**) The results of an immunofluorescent analysis of the PML distribution in the induced APL cells before and after treatment with ATRA. The images were captured with an LSM510 META confocal microscope (Carl Zeiss). All the bars indicate 10 μm. (**D, E**) The induction of myeloid differentiation in the induced APL cells by ATRA *in vivo*. The secondary recipients transplanted with the induced APL cells were then intraperitoneally treated with ATRA for 21 days. Cytospin slides of $EGFP^+/hCD45^+/hCD33^+$ cells from the secondary recipients transplanted with the induced APL cells are shown (**D**). The images were captured with a BX41 microscope (Olympus). The bar indicates 10 μm. Their differentiated cellular counts were evaluated, and the representative series data are indicated (**E**).
doi:10.1371/journal.pone.0111082.g004

they were transplanted intramedullary (iBM, 2.00% to 5.98%, n = 2) (**Figure 5A**). The immunophenotype of the engrafted cells was the same as that seen in the primary induced APL cells: they were positive for CD13 and CD33, without the expression of CD34 or HLA-DR (**Figure 5B**), demonstrating that the induced APL retains self-renewal capacity with a low level of transplan-

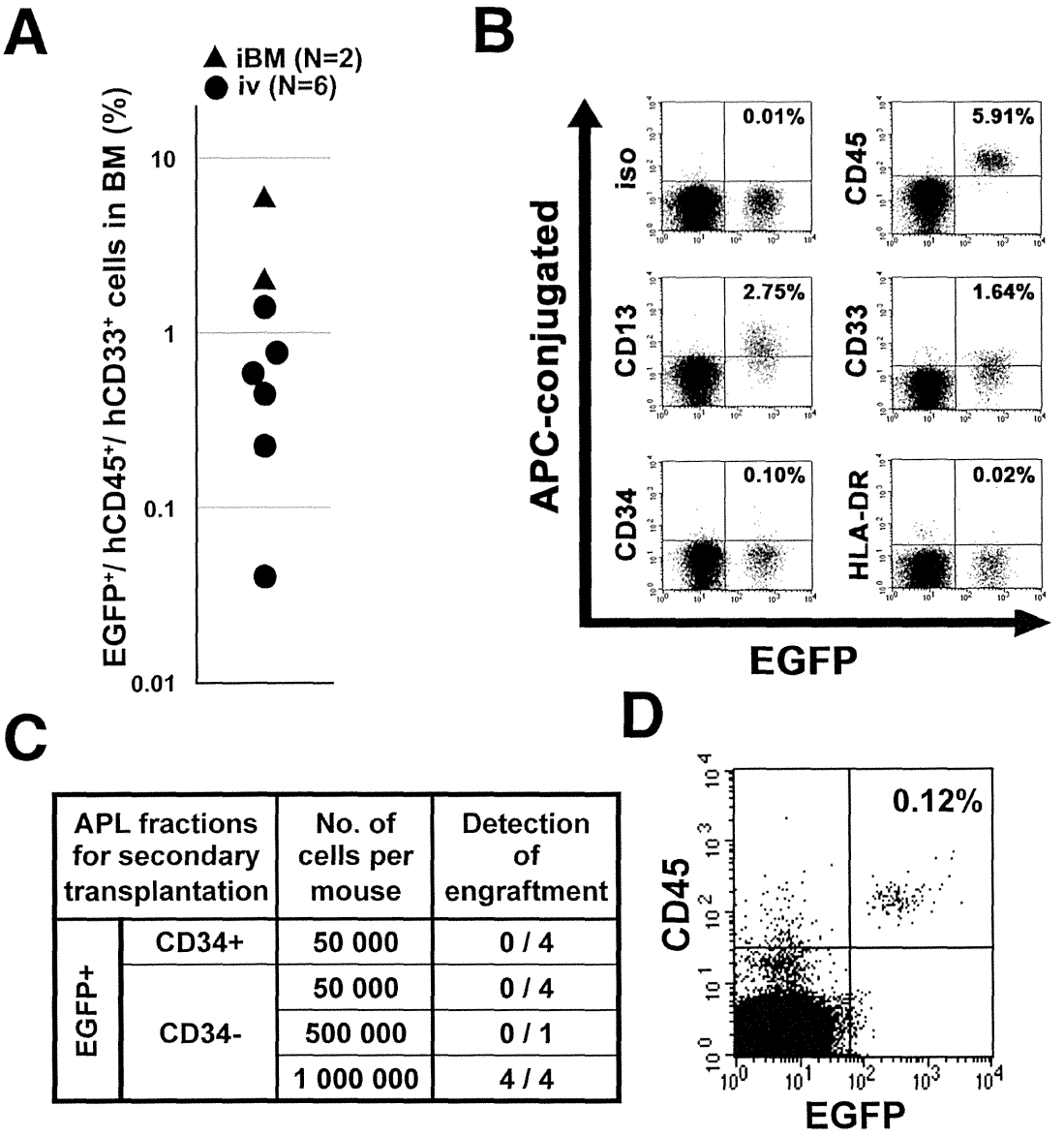

APL fractions for secondary transplantation		No. of cells per mouse	Detection of engraftment
EGFP+	CD34+	50 000	0 / 4
	CD34-	50 000	0 / 4
		500 000	0 / 1
		1 000 000	4 / 4

Figure 5. APL-LIC in the humanized APL *in vivo* model. (**A**) The engraftment of the induced APL cells in the secondary recipients. The bone marrow cells were obtained 16 weeks after transplantation and evaluated. Each dot represents a single mouse. (**B**) The immunophenotype of the induced APL cells in the secondary recipients. The representative pattern is shown. (**C**) The engraftment capacity in each fraction from the induced APL cells in the secondary recipients. The bone marrow cells were obtained 16 weeks after transplantation and evaluated. (**D**) The engraftment of the $CD34^-$ fraction in the secondary recipients. The engrafted cells are shown as $EGFP^+/CD45^+$ cells.
doi:10.1371/journal.pone.0111082.g005

tation efficiency. In addition, the results suggested that the capacity for engraftment in this xenograft model differed between the $CD34^+$ cells transduced with *PML-RARA* and the APL cells mostly composed of the $CD34^-$ fraction.

To identify a fraction responsible for the APL maintenance in the induced APL cases, $CD34^+$ and $CD34^-$ APL fractions were separately collected and transplanted intravenously. The $CD34^+$ fraction was pooled because there were very few $CD34^+$ cells in each induced APL case (**Figures 3A and 5B**). The $CD34^-$ fraction was sorted twice to exclude the $CD34^+$ fraction completely. Fifty thousand APL cells in both the $CD34^+$ and $CD34^-$ fractions failed to engraft in the secondary recipients (0 out of 4 mice in each fraction). Similar to the unsorted cells, one million $CD34^-$ fraction cells were able to engraft in recipient mice (4 out of 4 mice) (**Figures 5C and 5D**).

These findings revealed that $CD34^-$ induced APL cells exhibit the ability to function as APL-LIC *in vivo*, although the LIC function was not excluded in the $CD34^+$ APL fraction.

The $CD34^+/CD38^+$ progenitors trigger APL by *PML-RARA* induction *in vivo*

The findings that the *PML-RARA* transduced-$CD34^+$ cells developed APL while the resultant $CD34^-$ APL cells exhibited transplantability indicate the possibility that the initiation and maintenance of APL arise at different steps of differentiation, which are not likely to involve the $CD34^+/CD38^-$ fraction, as